Electronic Supplementary Material (ESI) for Journal of Materials Chemistry B.

Proteolytic functional amyloid digests pathogenic amyloid

Tanmay Mondal and Bhubaneswar Mandal*

Department of Chemistry, Indian Institute of Technology Guwahati, Assam-781039, India.

E-mail: bmandal@iitg.ac.in

ORCID

Tanmay Mondal: 0000-0002-3056-1955

Bhubaneswar Mandal: 0000-0003-3435-5443

The most stable conformation of PFAs:

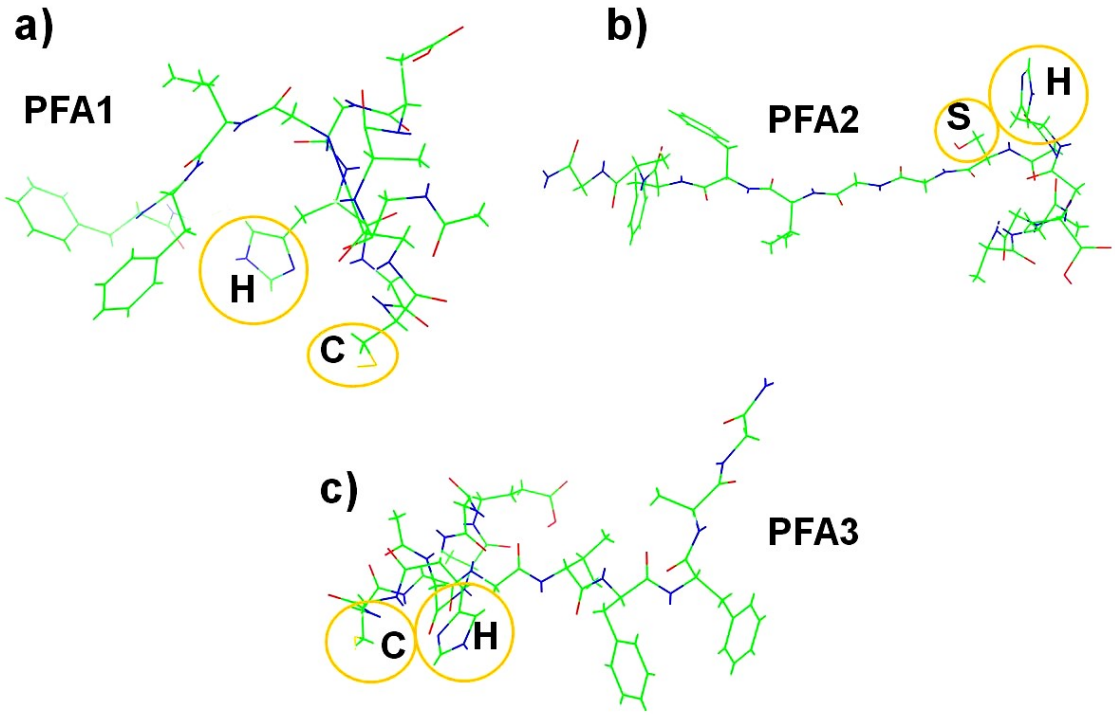

Figure S1. (a-c) The most stable conformation of PFA1-PFA3 respectively [image generated by PyMOL (Line representation)] obtained from DFT calculation [Calculation Method: B3LYP, Basis Set: 6-31G]. Nitrogen & Oxygen atoms are represented in blue & red, respectively.

Examination of the proteolytic activity of the PFAs on mAβ:

Self-degradation of mAβ:

Self-degradation of mAβ was described in the ESI (Fig. S17- S21) of our previously published article (*ChemComm* **2020**, 56, 2348-2351).

Self-degradation of Cys based PFA:

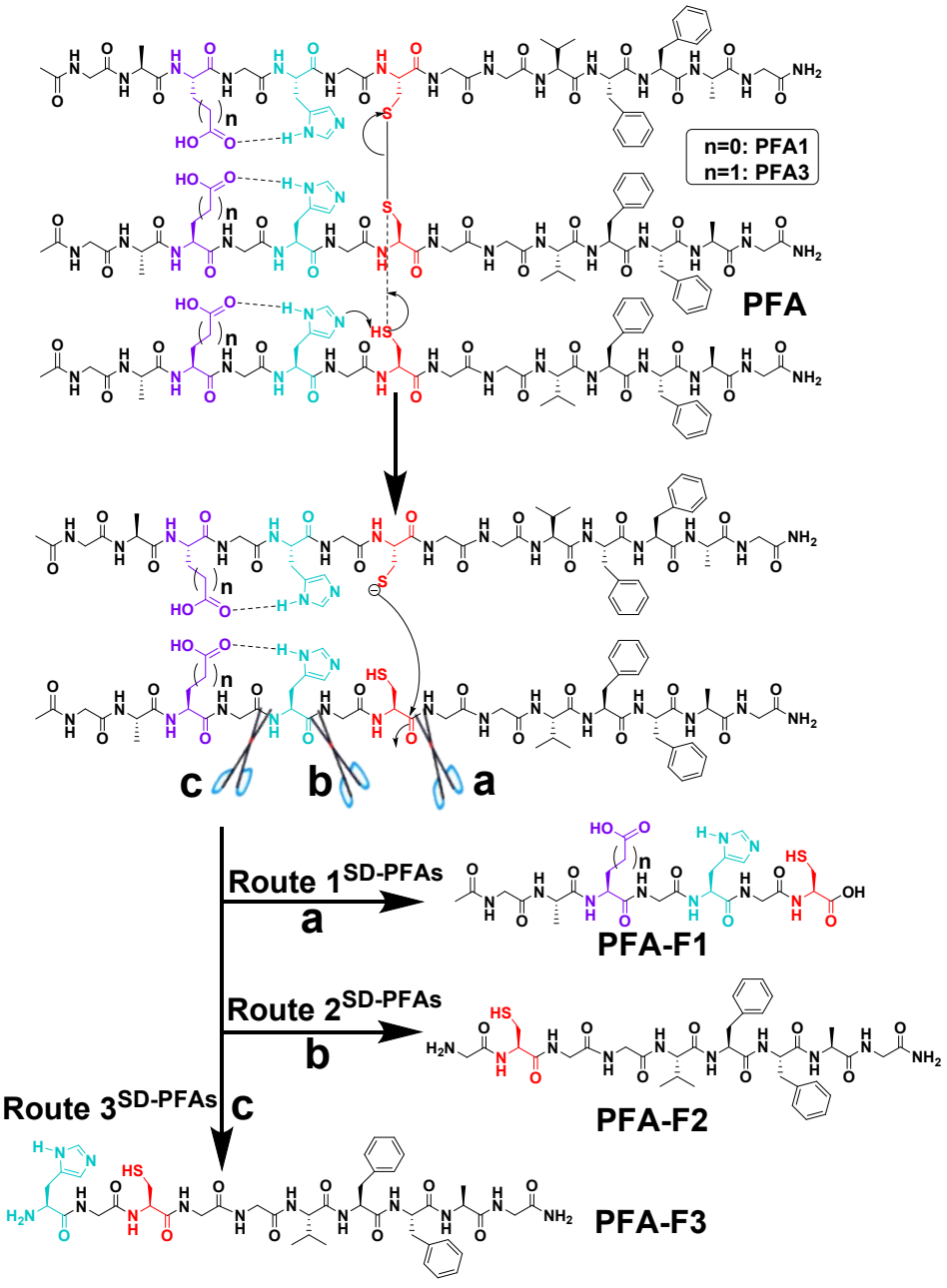

Figure S2. Plausible routes of the self-degradation of PFA.

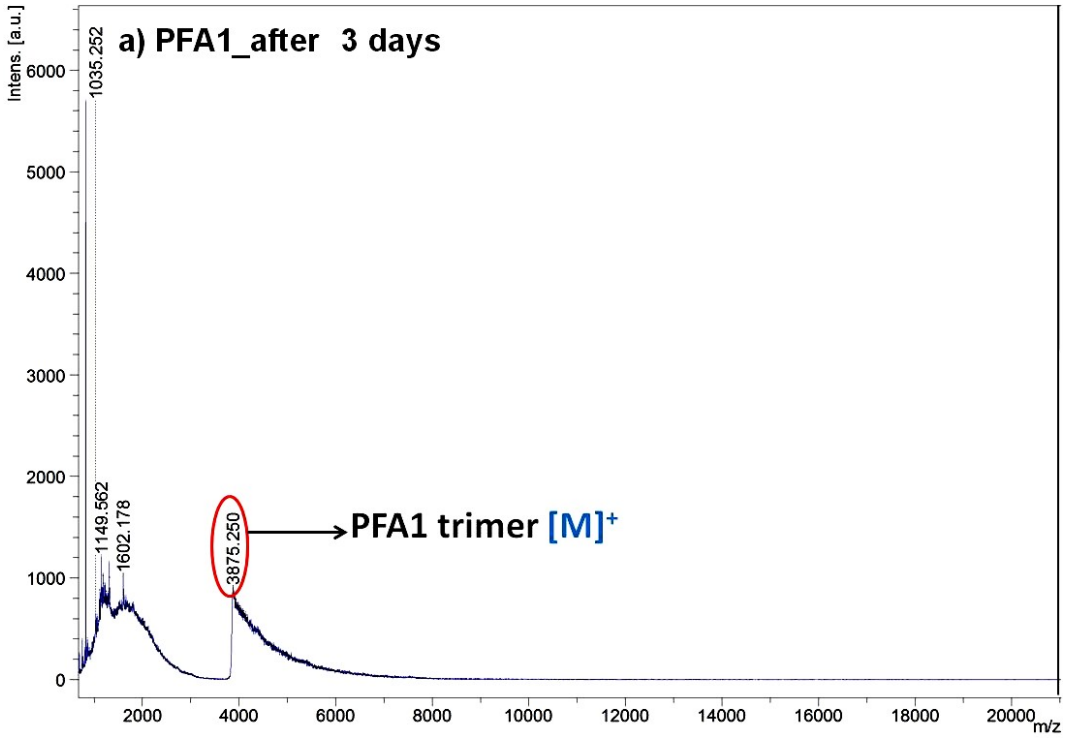

Figure S3. MALDI-TOF mass spectrum of PFA1 after three days of incubation.

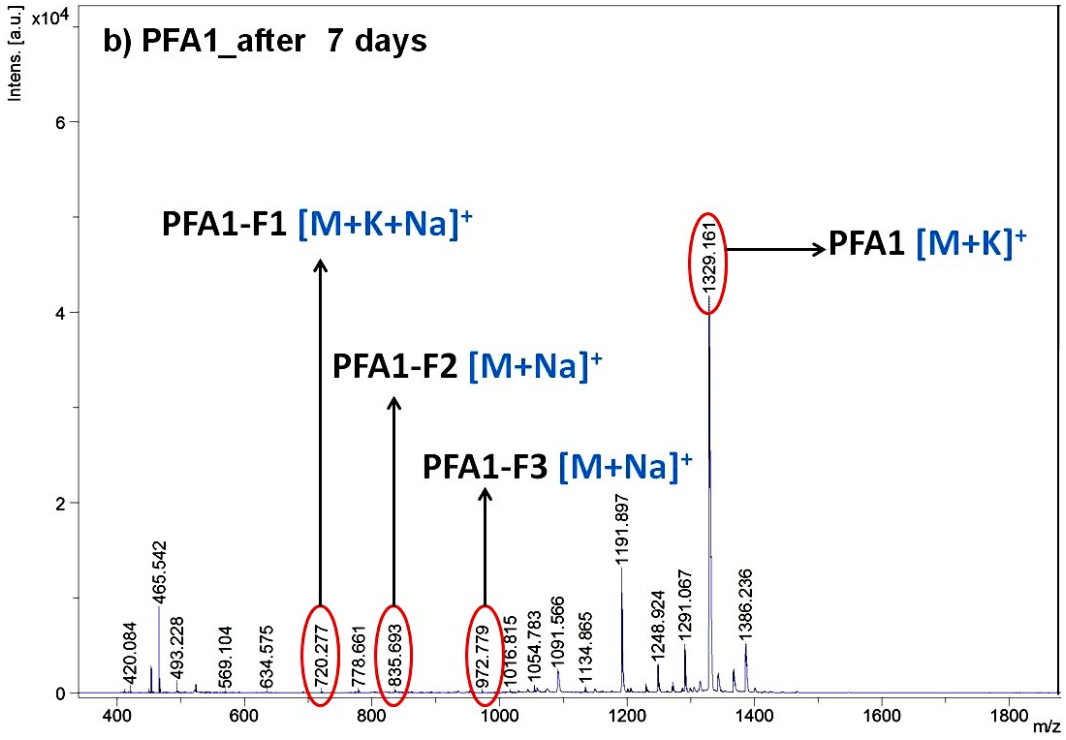

Figure S4. MALDI-TOF mass spectrum of PFA1 after seven days of incubation.

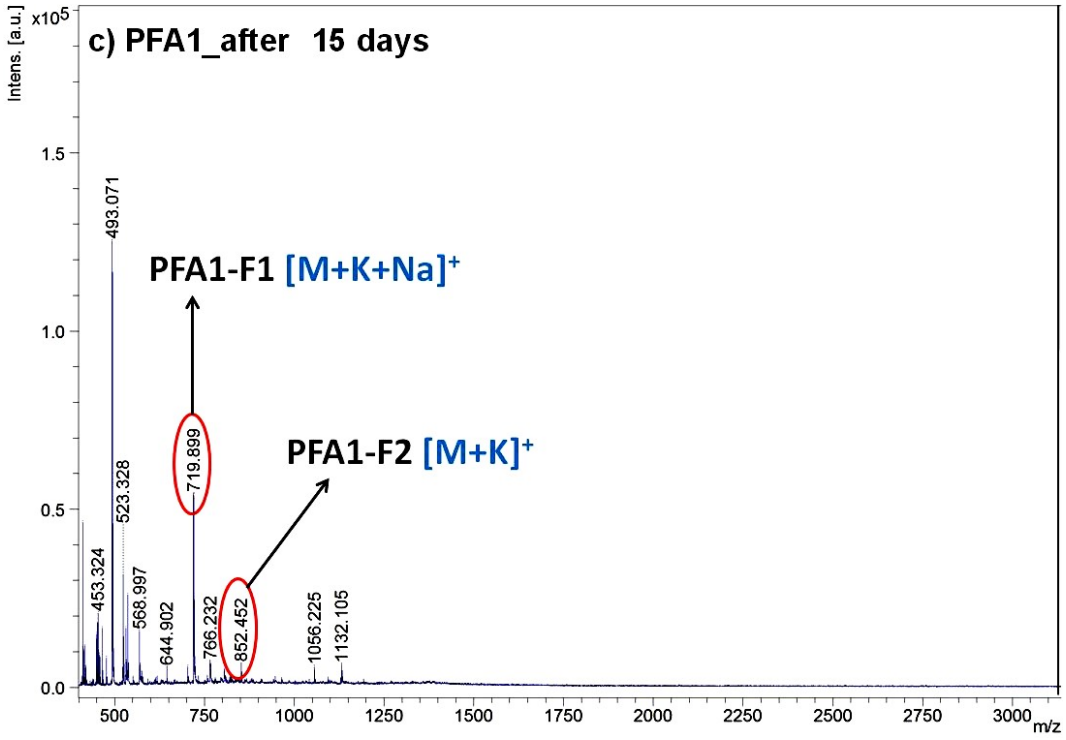

Figure S5. MALDI-TOF mass spectrum of PFA1 after 15 days of incubation.

Plausible mechanism of proteolysis by PFA:

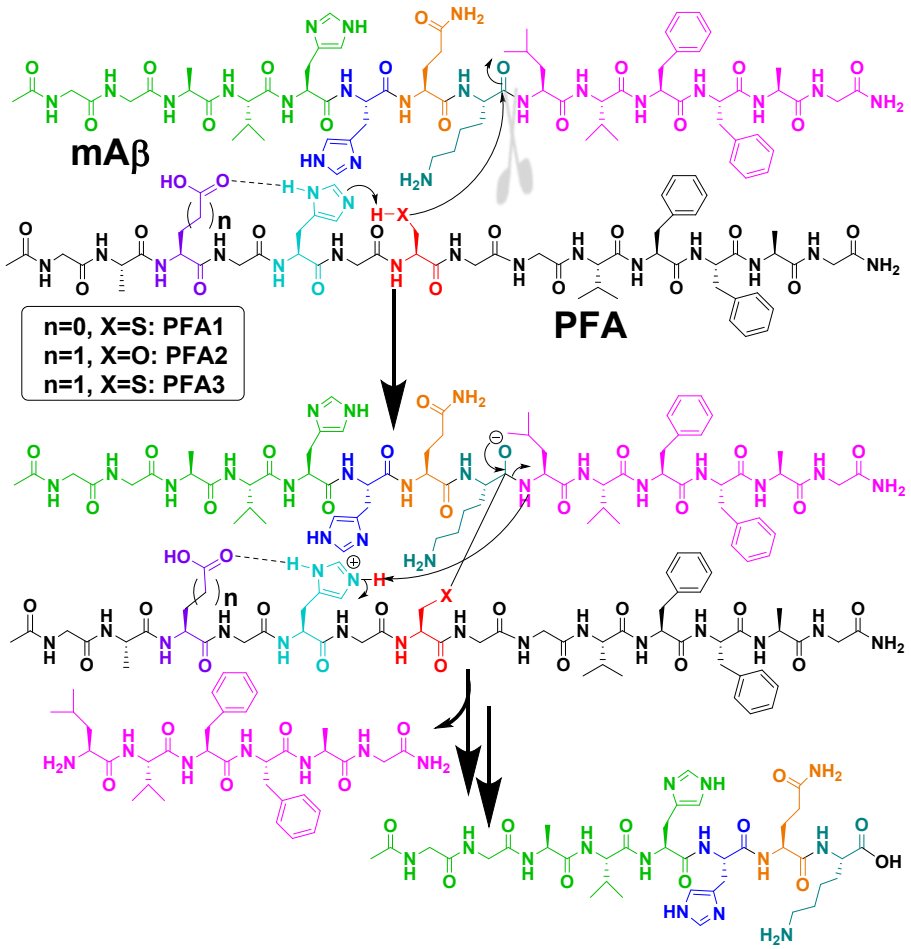

Figure S6. Plausible routes of the proteolysis of mAβ into various fragments by PFAs (Route 1$^{mAβ\text{-}PFAs}$).

Proteolytic activity of Cys based PFA on mAβ:

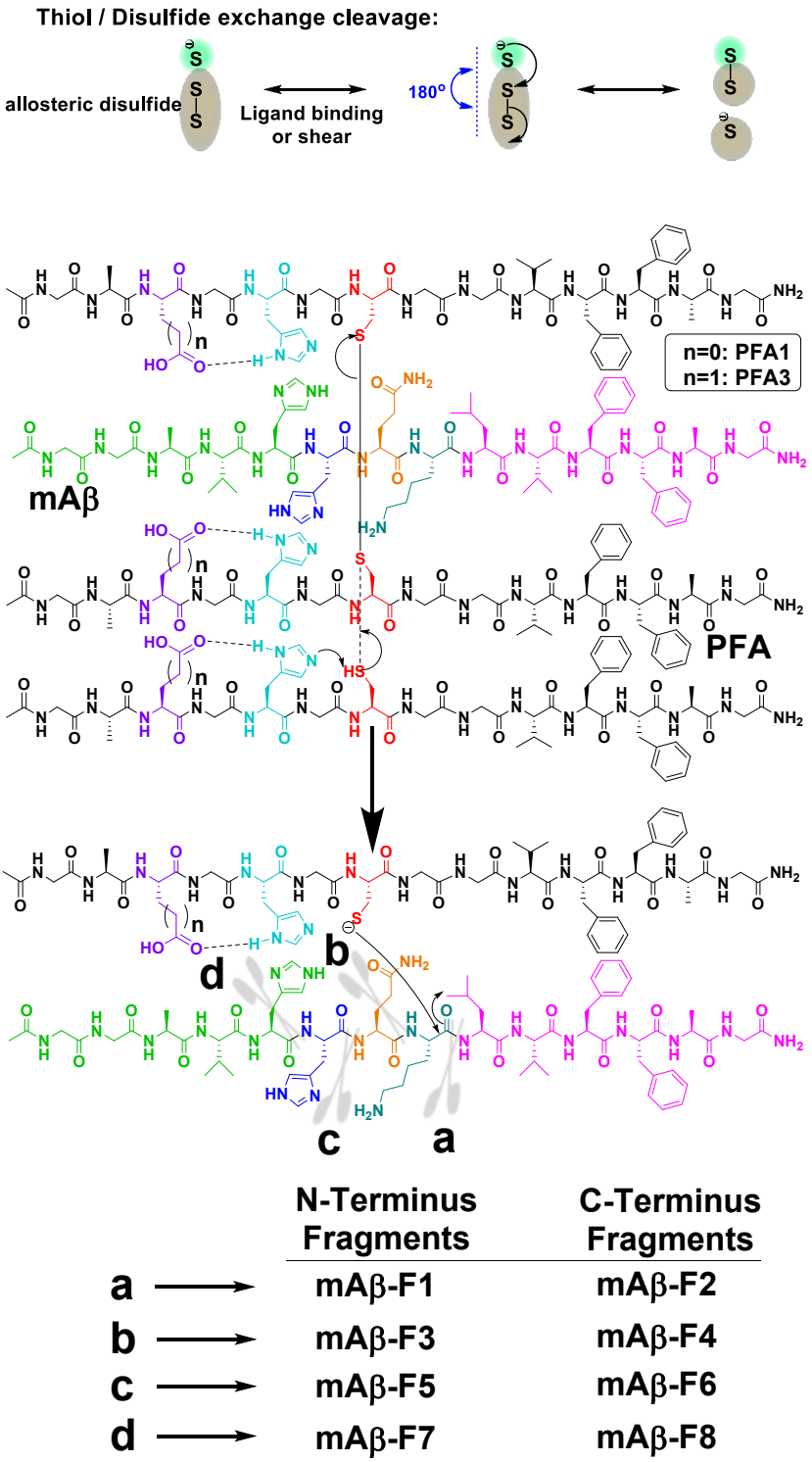

Figure S7. Thiol/ disulfide exchange cleavage to shear the adjacent protein. Plausible routes of the proteolysis of mAβ into various fragments by PFAs (Route 1$^{mAβ\text{-}PFAs}$).

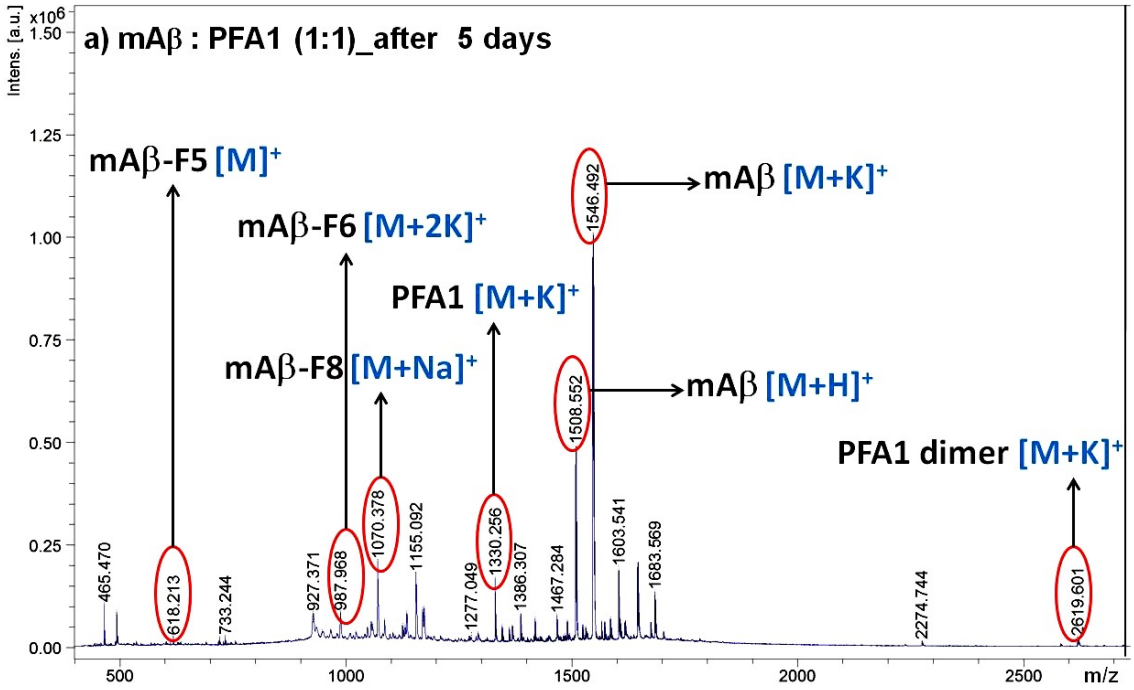

Figure S8. MALDI-TOF mass spectrum of mAβ in the presence of PFA1 (1:1) after five days of incubation.

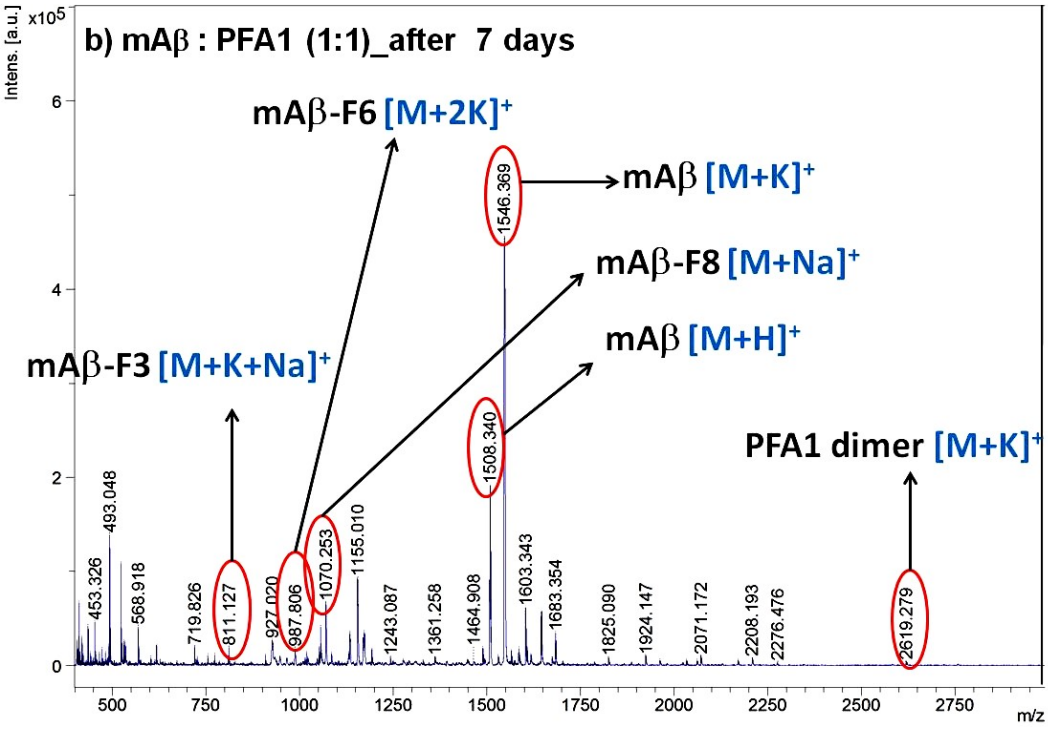

Figure S9. MALDI-TOF mass spectrum of mAβ in the presence of PFA1 (1:1) after five days of incubation.

Examination of the proteolytic activity of PFAs on $A\beta_{1-40}$:

Self-degradation of $A\beta_{1-40}$:

Self-degradation of Aβ1-40 was described in the ESI (Fig. S52- S54) of our published article (*ChemComm* **2020**, 56, 2348-2351).

Plausible routes of the proteolytic cleavage of $A\beta_{1-40}$ by PFAs:

Figure S10. Plausible routes of the proteolysis of $A\beta_{1-40}$ into various fragments by PFAs (Route $1^{A\beta\text{-}PFAs}$ - Route $7^{A\beta\text{-}PFAs}$).

Proteolytic activity of PFA1 on $A\beta_{1-40}$:

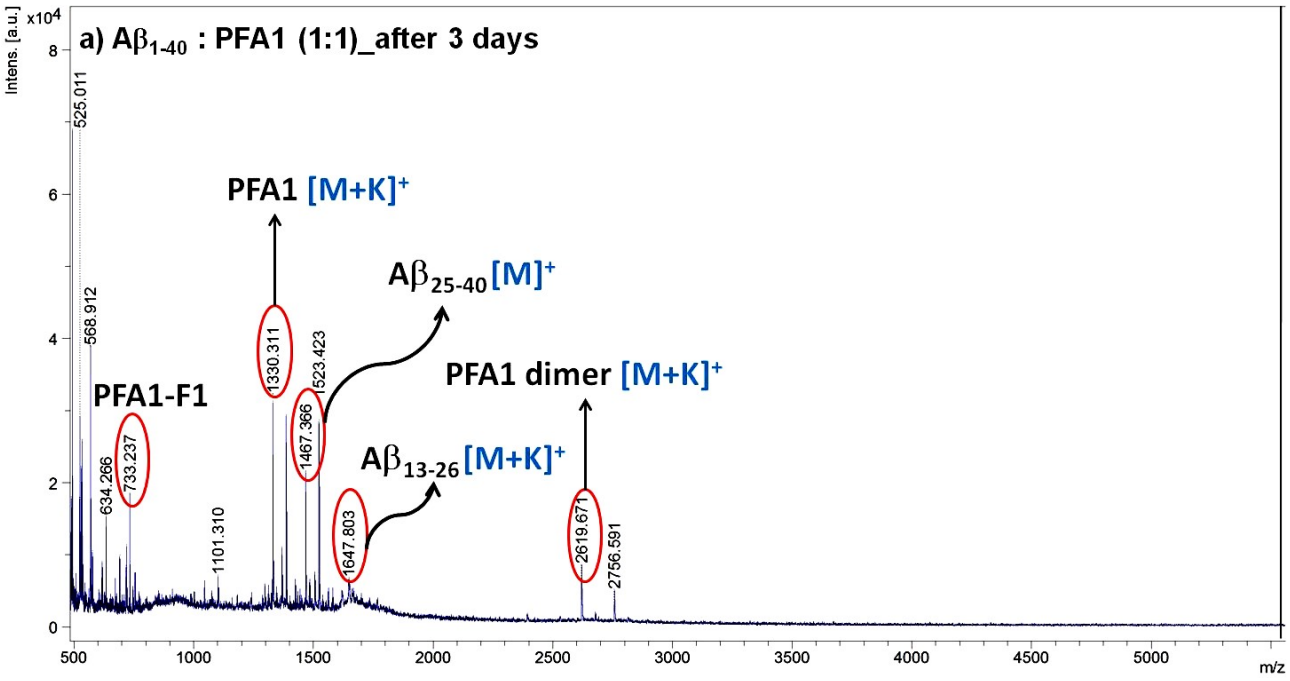

Figure S11. MALDI-TOF mass spectrum of $A\beta_{1-40}$ in the presence of PFA1 (1:1) after three days of incubation in PBS.

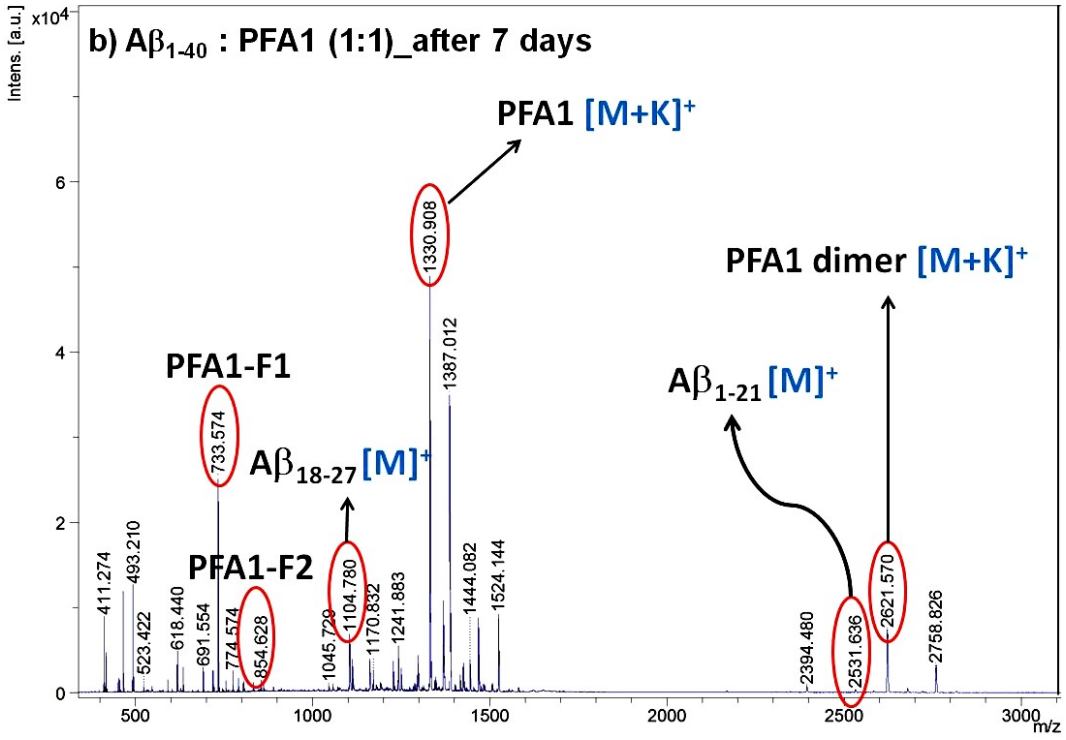

Figure S12. MALDI-TOF mass spectrum of $A\beta_{1-40}$ in the presence of PFA1 (1:1) after seven days of incubation in PBS.

Proteolytic activity of PFA2 on $A\beta_{1-40}$:

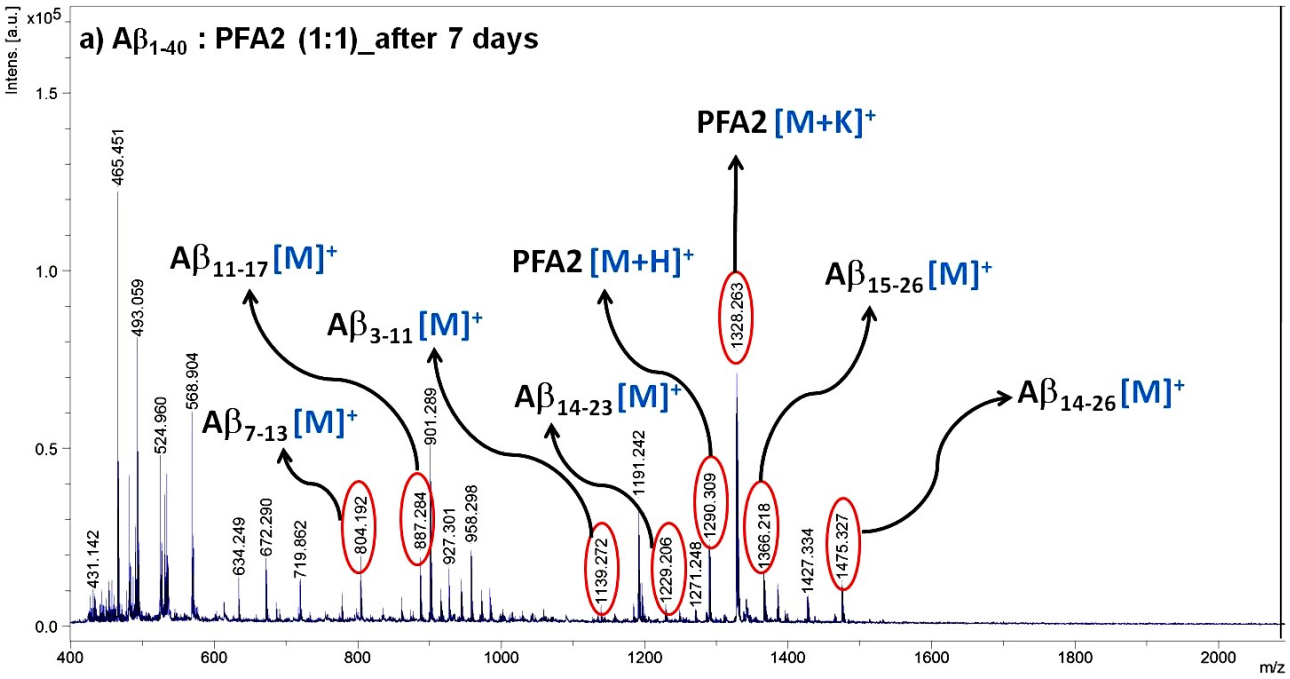

Figure S13. MALDI-TOF mass spectrum of $A\beta_{1-40}$ in the presence of PFA2 (1:1) after seven days.

Proteolytic activity of PFA3 on $A\beta_{1-40}$:

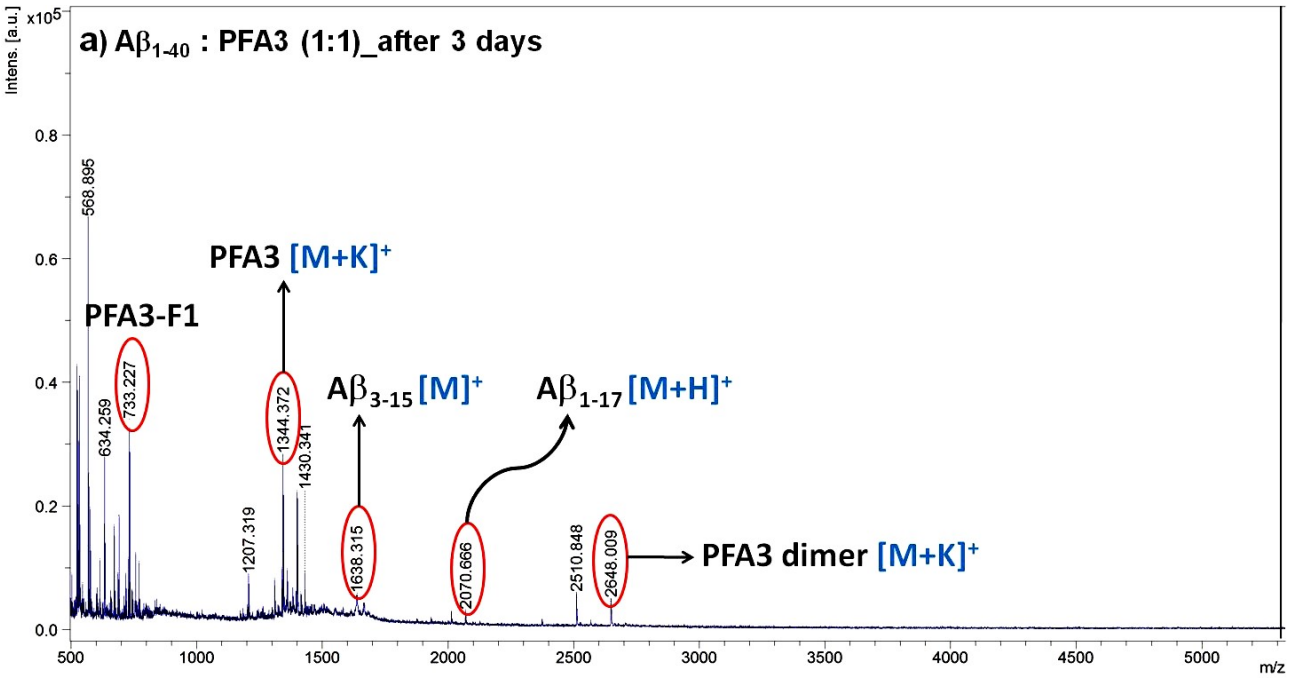

Figure S14. MALDI-TOF mass spectrum of $A\beta_{1-40}$ in the presence of PFA3 (1:1) after three days of incubation in PBS.

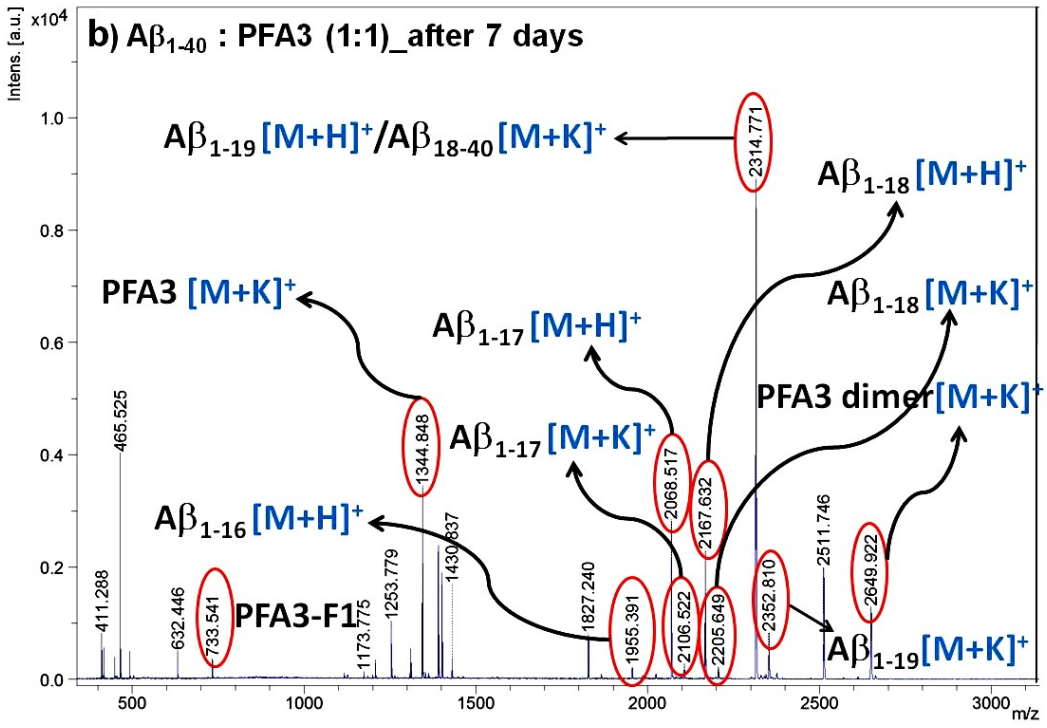

Figure S15. MALDI-TOF mass spectrum of $A\beta_{1-40}$ in the presence of PFA3 (1:1) after seven days.

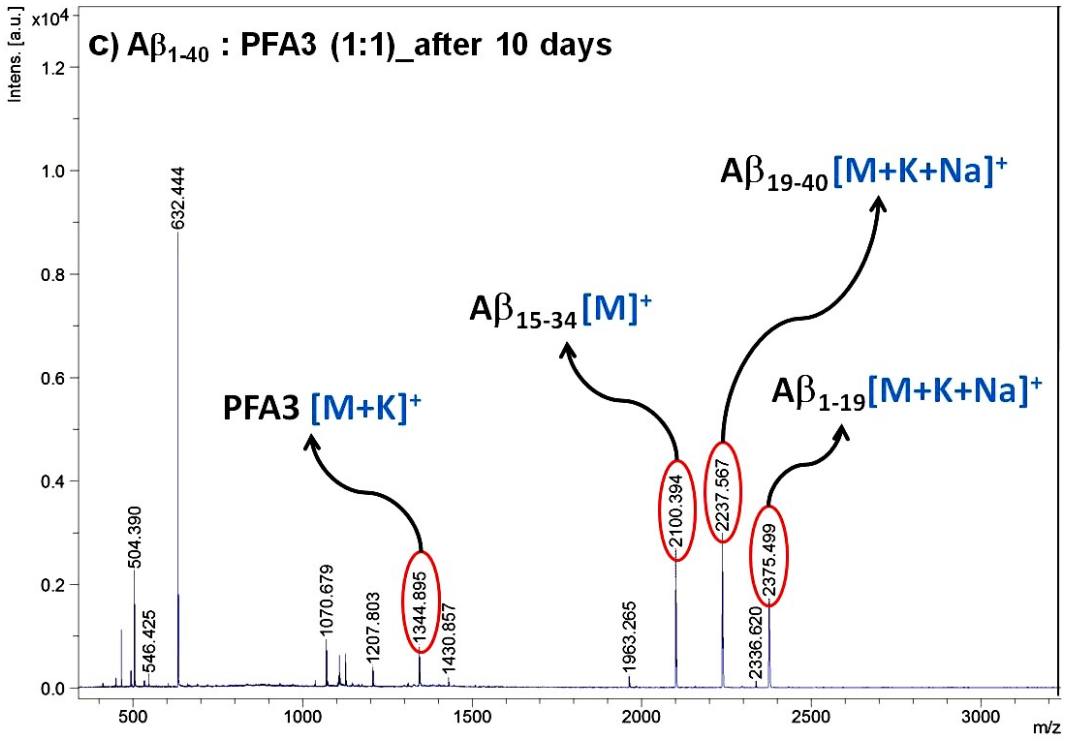

Figure S16. MALDI-TOF mass spectrum of $A\beta_{1-40}$ in the presence of PFA3 (1:1) after ten days of incubation in PBS.

Examination of the proteolytic activity of PFA3 on DTP28:

Self-degradation of DTP28 was described in the ESI (Fig. S75- S79) of our published article (*ChemComm* **2020**, 56, 2348-2351).

Effect of PFA3 on the negative control (NC) peptide, DTP28:

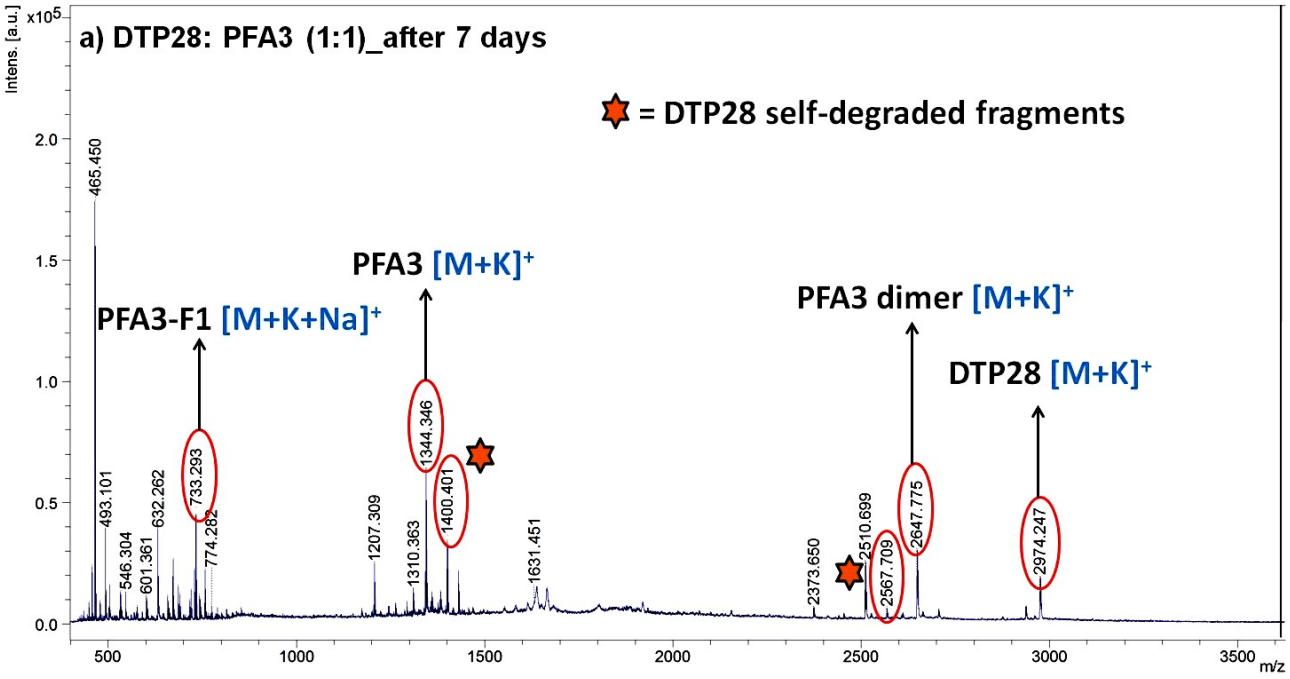

Figure S17. MALDI-TOF mass spectrum of NC (DTP28) in the presence of PFA3 (1:1) after seven days of incubation in PBS.

Inhibitory ability of EGCG on mAβ:

MALDI-TOF mass spectra of mAβ in the presence of EGCG were analysed in a time-dependent manner. However, PFAs mediated no such degradation product was observed in mass spectra, a few self-degraded peptide fragments were appeared due to the inhibition of mAβ by EGCG.

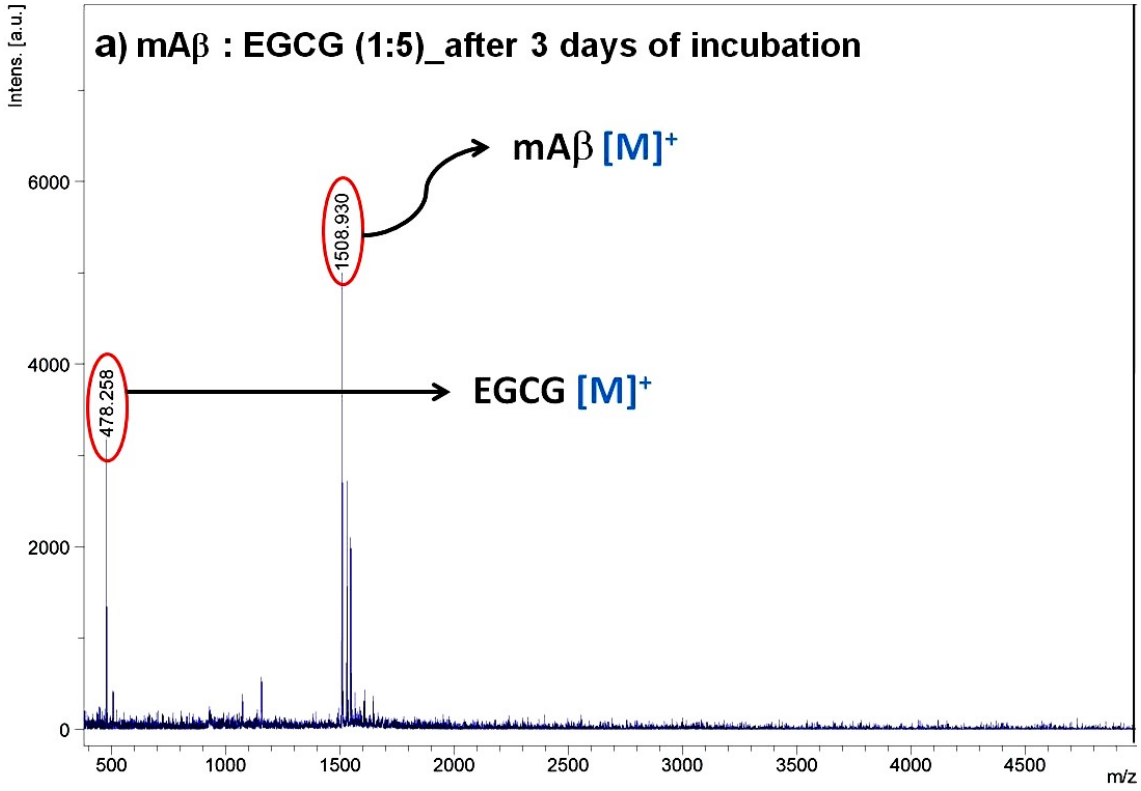

Figure S18. MALDI-TOF mass spectrum of mAβ in the presence of EGCG (1:5) after three days of incubation at the physiological condition.

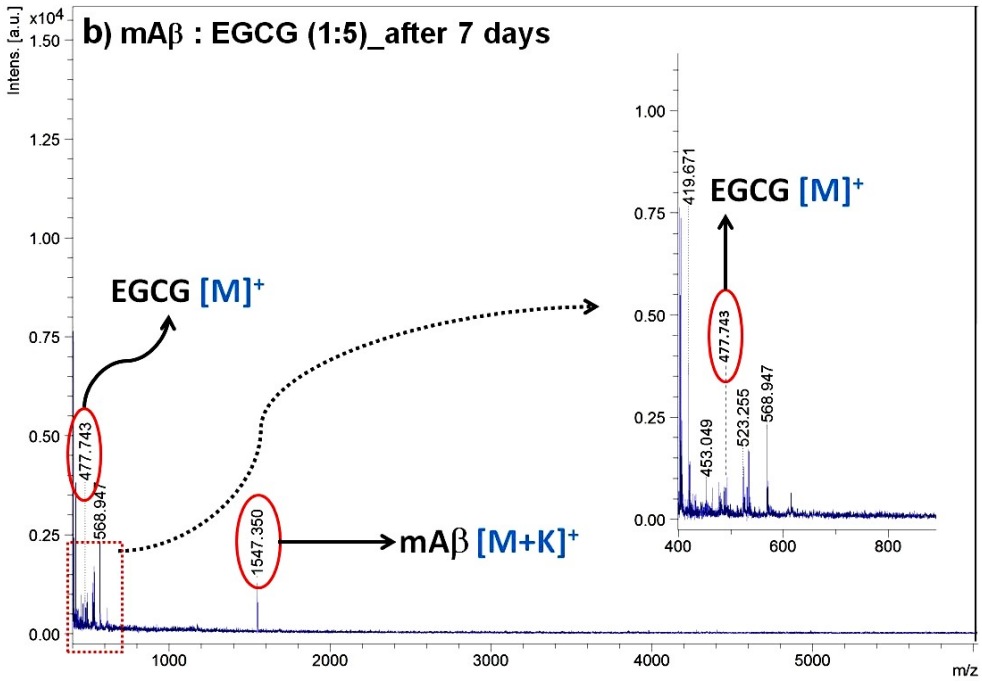

Figure S19. MALDI-TOF mass spectrum of mAβ in the presence of EGCG (1:5) after seven days. PFAs mediated no such degradation product was observed in the spectrum, though a few self-degraded peptide fragments were appeared due to the inhibition of mAβ by EGCG.

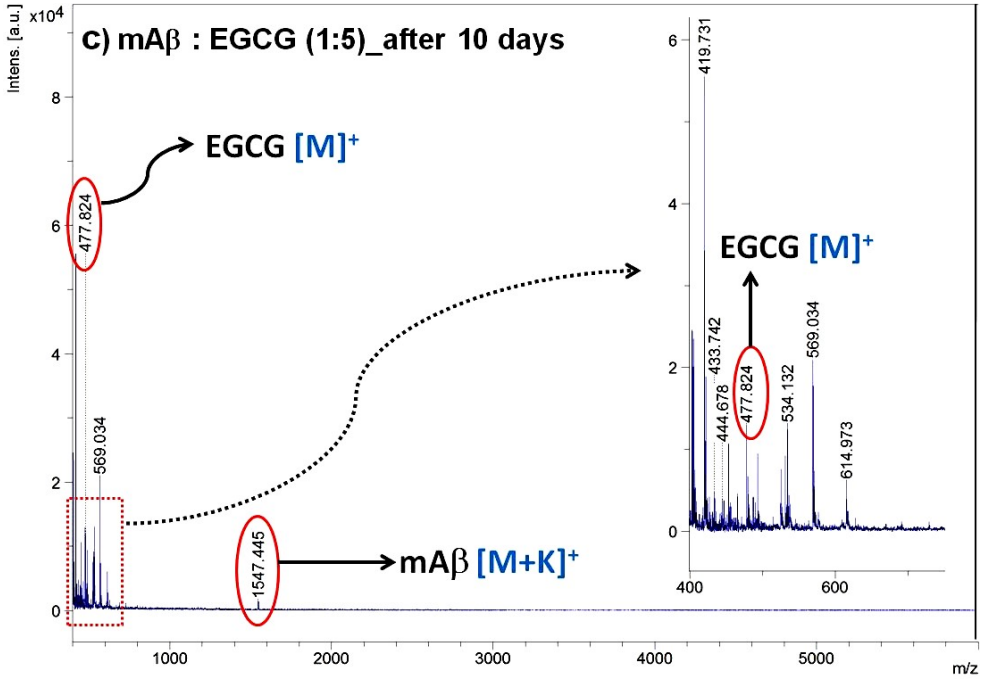

Figure S20. MALDI-TOF mass spectrum of mAβ in the presence of EGCG (1:5) after ten days. PFAs mediated no such degradation product was observed in the spectrum, though a few self-degraded peptide fragments were appeared due to the inhibition of mAβ by EGCG.

Fluorescence resonance energy transfer (FRET) assay:

Overlap of the emission spectrum of donor-peptide FmAβ1 and the absorbance spectrum of acceptor-peptide FmAβ2 was found to be similar as reported in our published article (*ChemComm* **2020**, 56, 2348-2351).

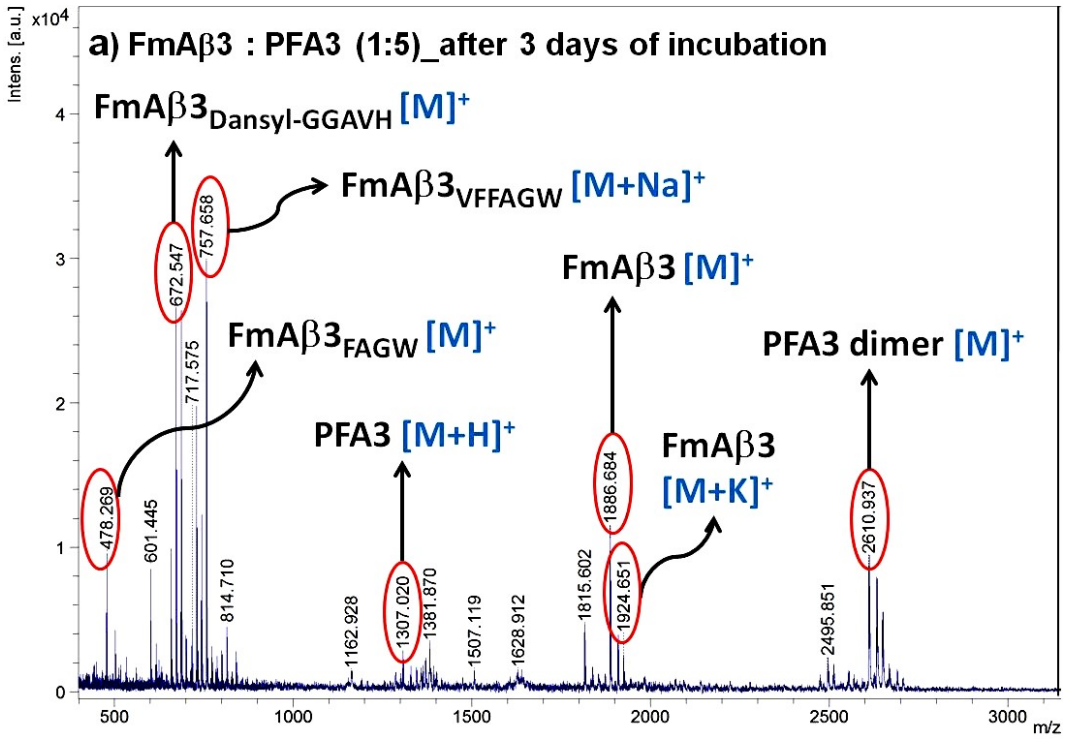

Figure S21. MALDI-TOF mass spectrum of FmAβ3 in the presence of five-fold PFA3 after three days of incubation in PBS pH 7.4 at 37 °C.

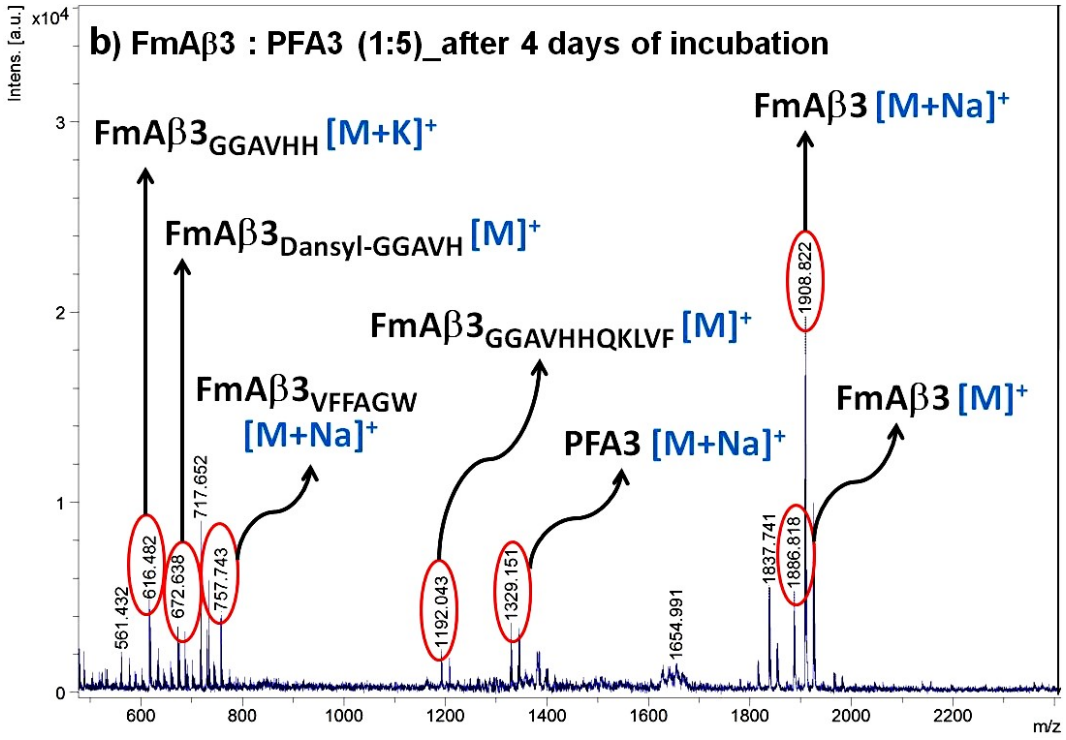

Figure S22. MALDI-TOF mass spectrum of FmAβ3 in the presence of five-fold PFA3 after four days.

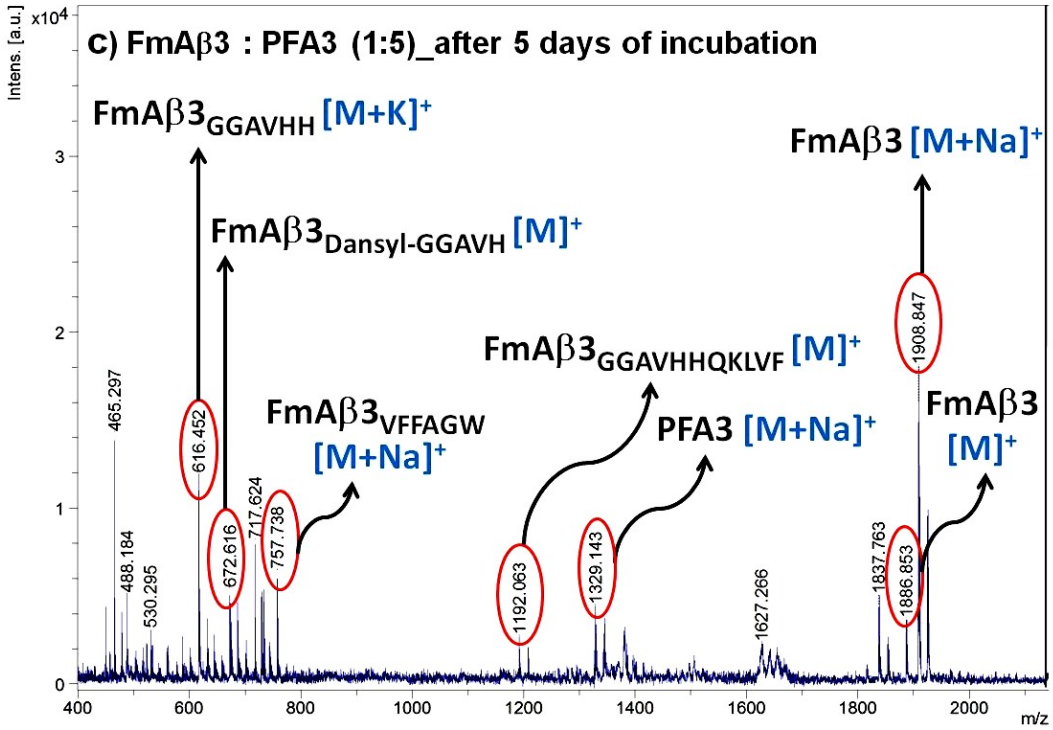

Figure S23. MALDI-TOF mass spectrum of FmAβ3 in the presence of five-fold PFA3 after five days.

Kinetics of the PFA3-catalyzed hydrolysis of p-Nitrophenyl Acetate (NPA):

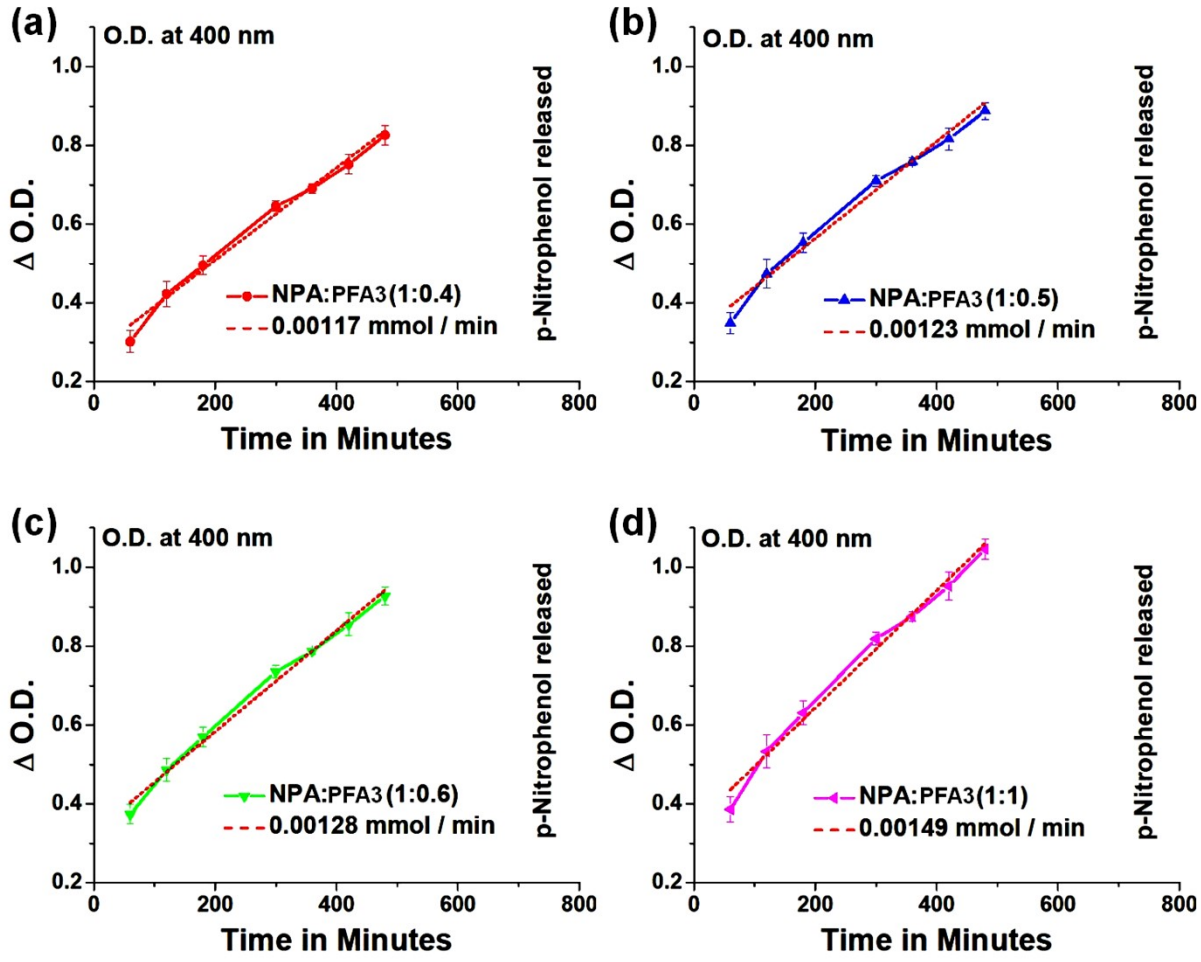

Figure S24. The relationship between the increase in absorbance at 400 nm and time in the hydrolysis of NPA (1 mM) by (a) 0.4 eq. PFA3, (b) 0.5 eq. PFA3, (c) 0.6 eq. PFA3, and (d) 1.0 eq. PFA3 in PBS buffer (containing 2 vol% ethanol) of pH 7.0 at 25 °C.

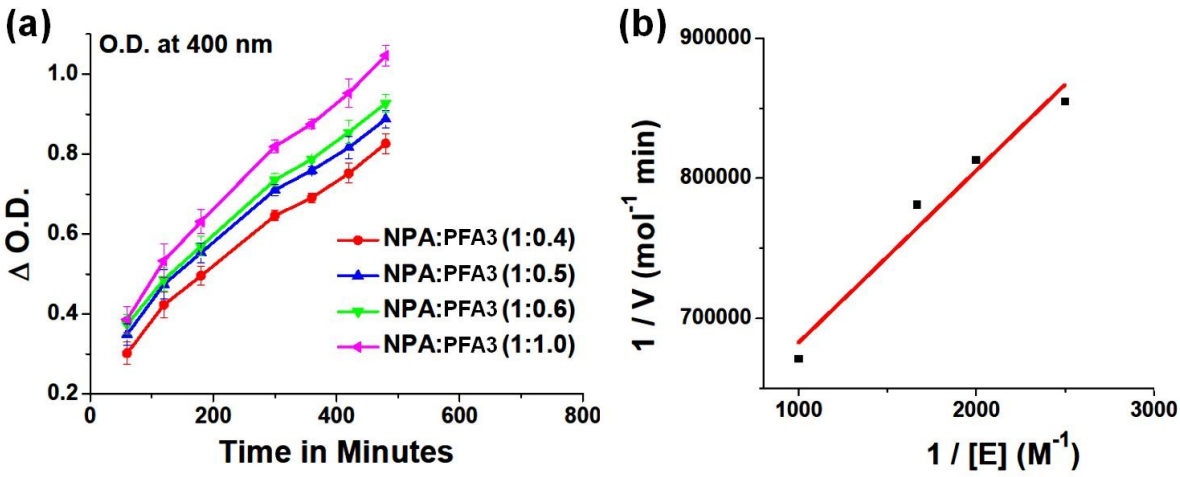

Figure S25. (a) The relationship between the increase in absorbance at 400 nm and time in the hydrolysis of NPA (1 mM) by PFA3 in PBS buffer (containing 2 vol% ethanol) of pH 7.0 at 25 °C. The Turn Over Number (T.O.N.) was calculated as moles hydrolyzed/min/moles of the enzyme. So, T.O.N. = 0.00149/0.001 = 1.49 [As assay volume is 1 mL, no. of moles of PFA3 = (1 mol/L) x 1 x 10^{-3} L]. (b) The Lineweaver-Burk plot of PFA3-catalyzed hydrolysis of NPA (Adj. R-Square: 0.95002).

Molecular Docking:

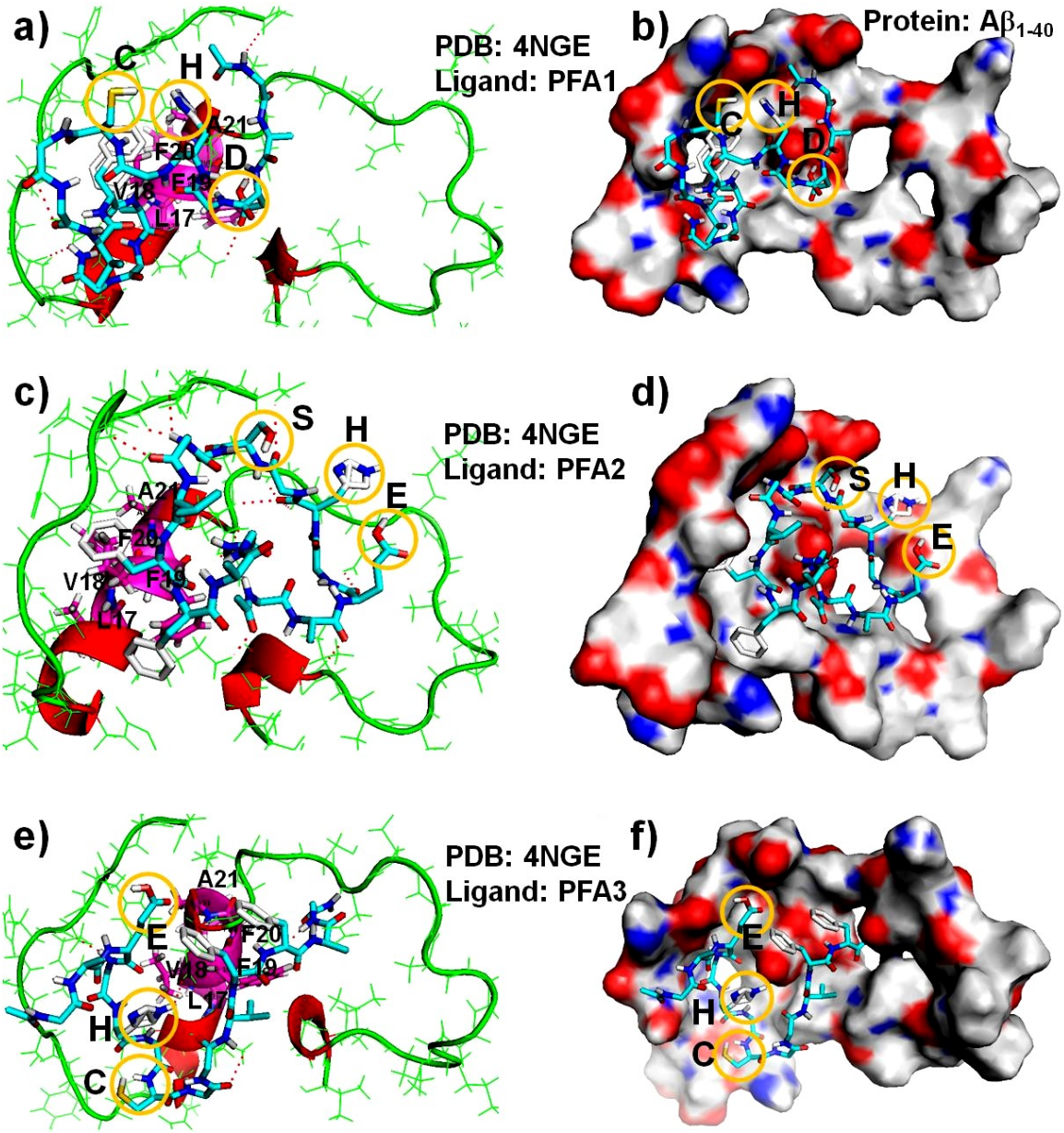

Figure S26. Molecular docking images of PFA1 (a, b), PFA2 (c, d), and PFA3 (e, f) into helical $A\beta_{1-40}$ (PDB ID 4NGE) reveals that PFAs bind at the binding site ($V_{18}FFA_{21}$) with binding affinity -6.1 kcal/mol, -6.1 kcal/mol , and -6.2 kcal/mol, respectively. Structures are shown as line and cartoon representation (for a, c, e), and surface representation (for b, d, f). The surface of $A\beta_{1-40}$ is coloured according to the charges of the atoms where negatively and positively charged zones are represented in red and blue, respectively.

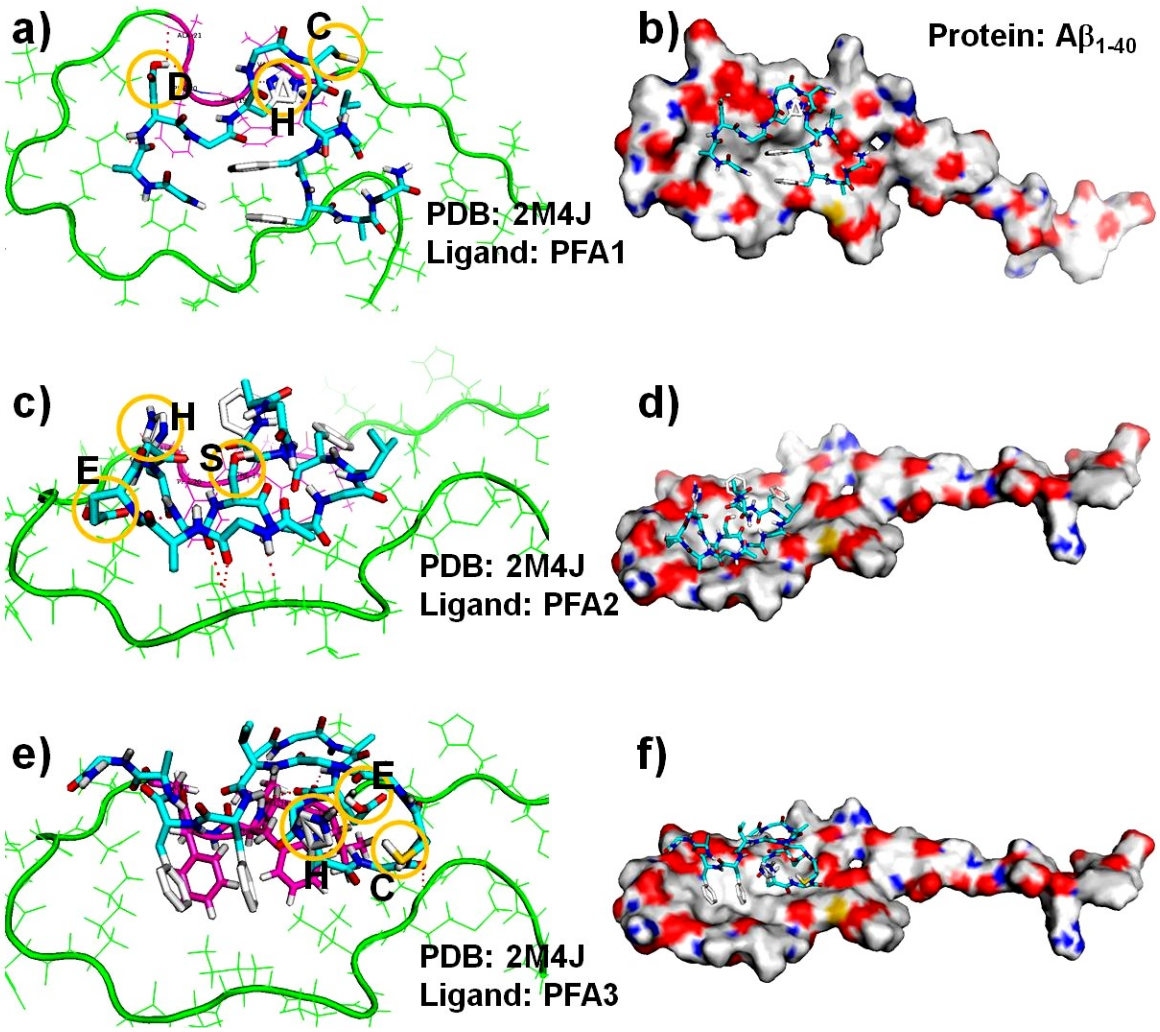

Figure S27. Molecular docking images of PFA1 (a, b), PFA2 (c, d), and PFA3 (e, f) into fibril $A\beta_{1-40}$ (PDB ID 2M4J) reveals that PFAs bind at the binding site ($V_{18}FFA_{21}$) with binding affinity -4.8 kcal/mol, -4.0 kcal/mol , and -5.2 kcal/mol, respectively. Structures are shown as line and cartoon representation (for a, c, e), and surface representation (for b, d, f). The surface of $A\beta_{1-40}$ is coloured according to the charges of the atoms where negatively and positively charged zones are represented in red and blue, respectively.

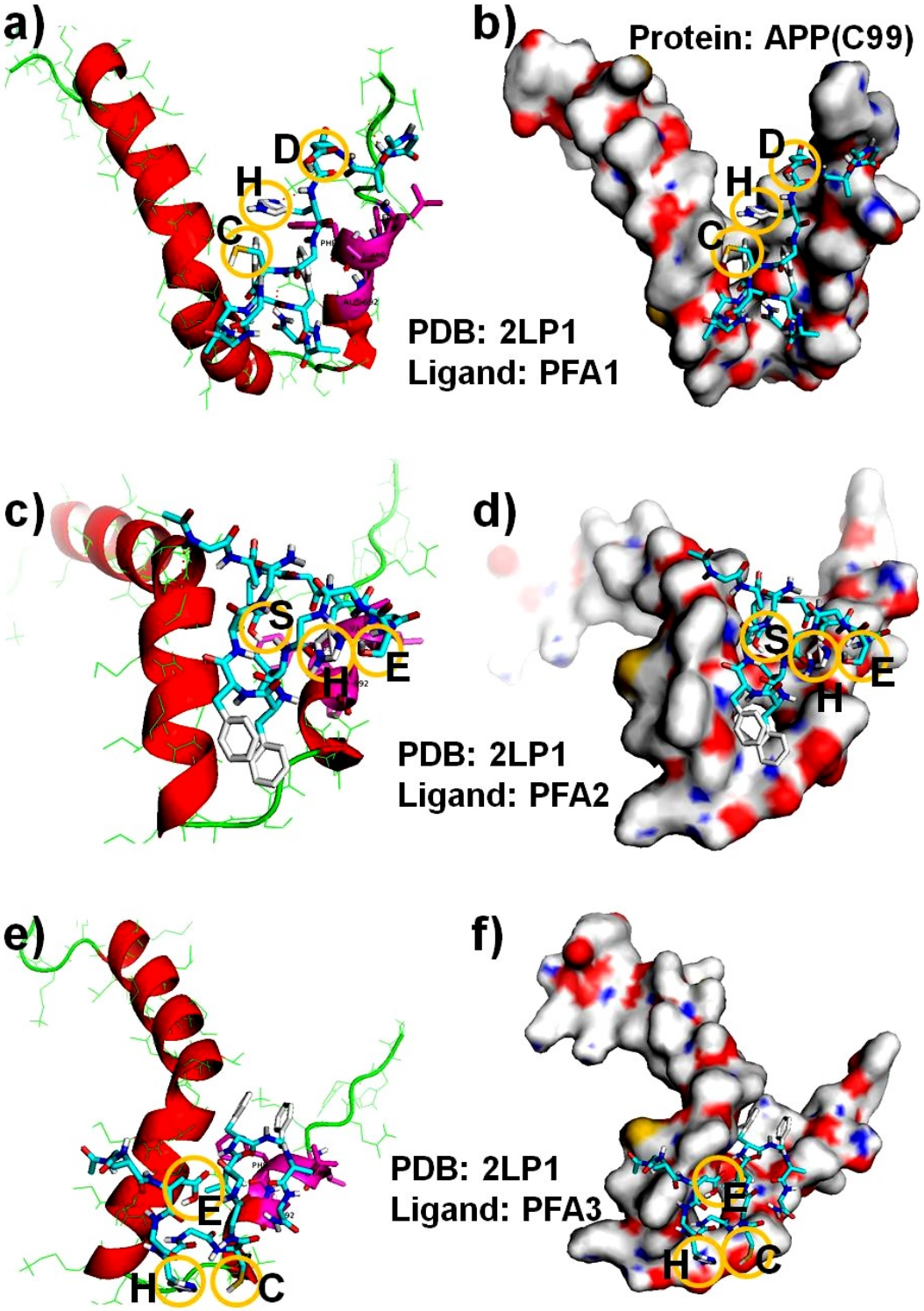

Figure S28. Molecular docking images of PFA1 (a, b), PFA2 (c, d), and PFA3 (e, f) into helical 99 residues C-terminal domain (PDB ID: 2LP1) of APP(C99) reveals that PFAs bind at the binding site ($V_{18}FFA_{21}$) with binding affinity -4.4 kcal/mol, -4.7 kcal/mol , and -5.5 kcal/mol, respectively. Structures are shown as line and cartoon representation (for a, c, e), and surface representation (for b, d, f). The surface of $A\beta_{1-40}$ is coloured according to the charges of the atoms where negatively and positively charged zones are represented in red and blue, respectively.

Inhibition of amyloid accumulation of $A\beta_{1-40}$ by PFA1:

ThT fluorescence assay, CD experiments, and FTIR spectra of $A\beta_{1-40}$:

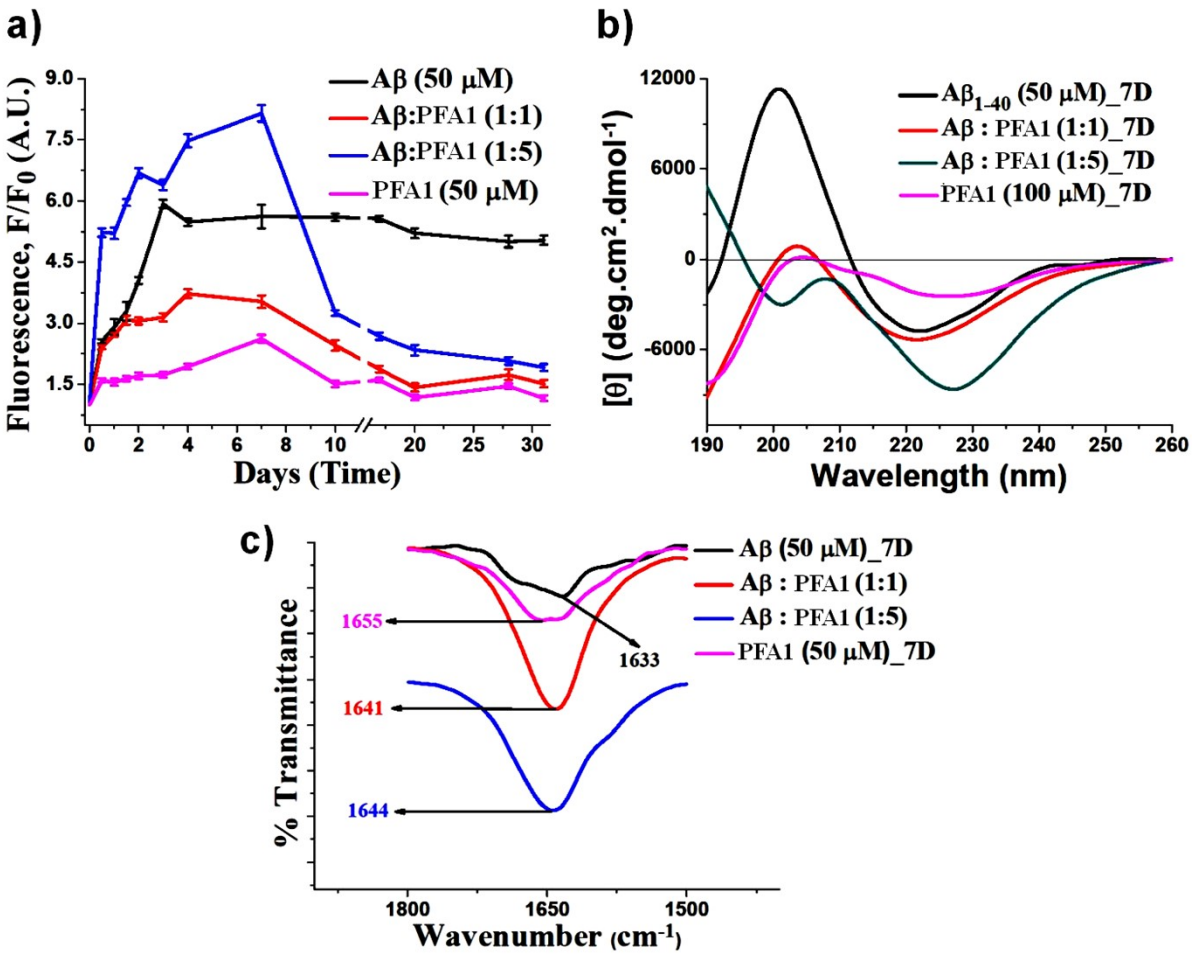

Figure S29. Normalized profiles of (a) dose-dependent ThT fluorescence assay. Spectra of $A\beta_{1-40}$ in the absence (black), presence of one-fold PFA1 (red), five-fold PFA1 (blue), and PFA1 alone (magenta). Error bars represent standard deviations of at least three independent measurements. (b) CD spectra of $A\beta_{1-40}$ in the absence and presence of PFA1 after seven days of incubation. Spectra of $A\beta_{1-40}$ in the absence (black), presence of one-fold PFA1 (red), five-fold PFA1 (dark cyan), and PFA1 alone (magenta). (c) FTIR spectra of $A\beta_{1-40}$ in the absence and presence of PFA1 after seven days of incubation. Spectra of $A\beta_{1-40}$ in the absence (black), presence of one-fold (red) PFA1, five-fold PFA1 (blue), and PFA1 alone (magenta). All the peptide solutions were incubated in PBS pH 7.4 (50 mM) at 37 °C.

TEM images and Congo red-stained birefringence images of amyloid fibrils formed by $A\beta_{1-40}$:

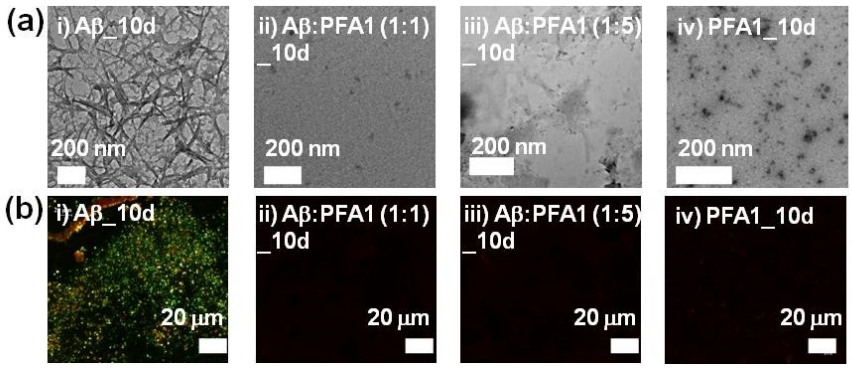

Figure S30. (a) TEM images, and (b) Congo red-stained birefringence images of $A\beta_{1-40}$ (i) in the absence, and presence of (ii) one-fold PFA1, (iii) five-fold PFA1, and (iv) PFA1 alone. Scale bars are indicated as 200 nm for TEM images, and 20 μm for birefringence images. All the peptide solutions were incubated in PBS pH 7.4 (50 mM) at 37 °C in parallel. All the images were captured after ten days of incubation.

Inhibition of amyloid accumulation of $A\beta_{1-40}$ by PFA2:

ThT fluorescence assay, CD experiments, and FTIR spectra of $A\beta_{1-40}$:

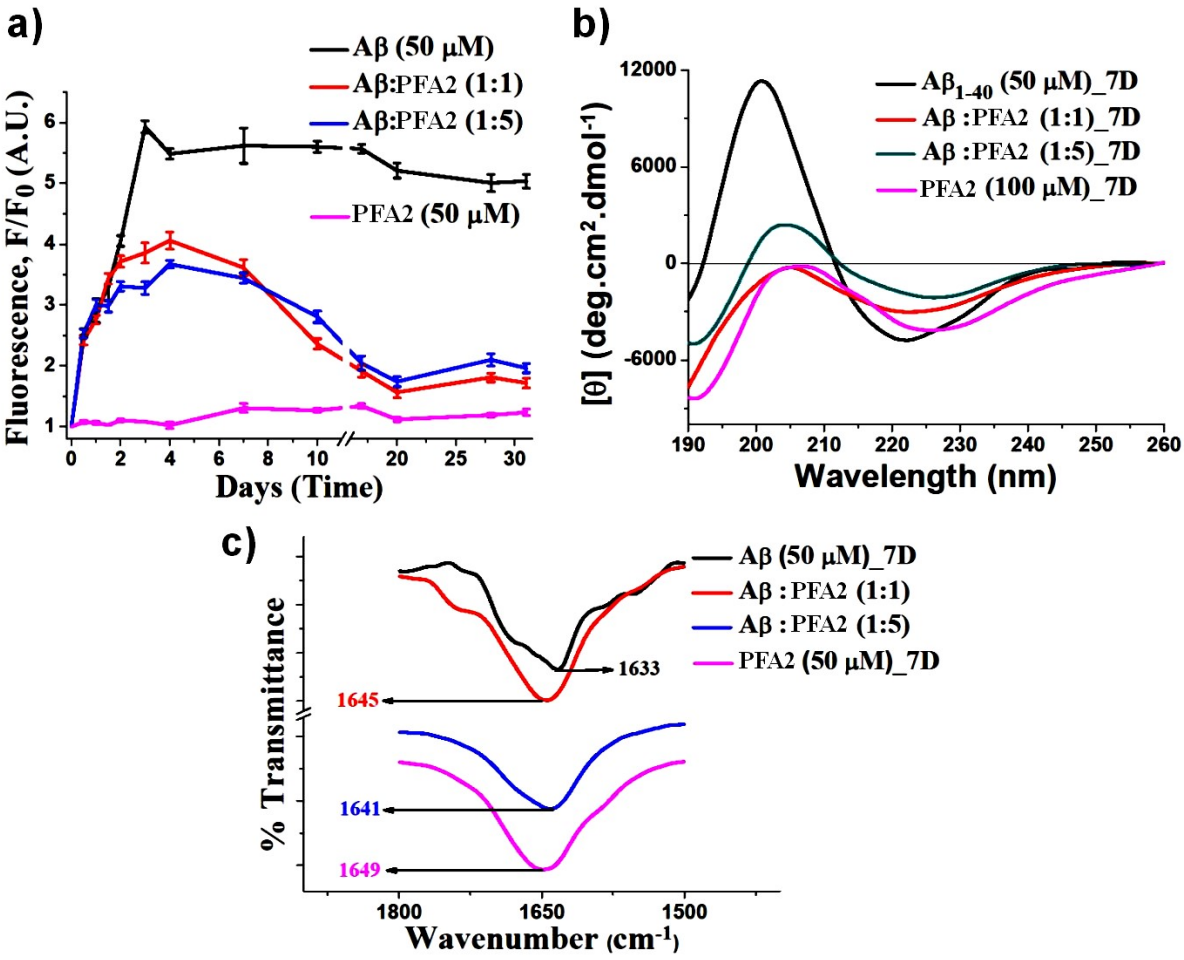

Figure S31. Normalized profiles of (a) dose-dependent ThT fluorescence assay. Spectra of $A\beta_{1-40}$ in the absence (black), presence of one-fold PFA2 (red), five-fold PFA2 (blue), and PFA2 alone (magenta). Error bars represent standard deviations of at least three independent measurements. (b) CD spectra of $A\beta_{1-40}$ in the absence and presence of PFA2 after seven days of incubation. Spectra of $A\beta_{1-40}$ in the absence (black), presence of one-fold PFA2 (red), five-fold PFA2 (dark cyan), and PFA2 alone (magenta). (c) FTIR spectra of $A\beta_{1-40}$ in the absence and presence of PFA2 after seven days of incubation. Spectra of $A\beta_{1-40}$ in the absence (black), presence of one-fold (red) PFA2, five-fold PFA2 (blue), and PFA2 alone (magenta). All the peptide solutions were incubated in PBS pH 7.4 (50 mM) at 37 °C.

TEM images, and Congo red-stained birefringence images of amyloid fibrils formed by $A\beta_{1-40}$:

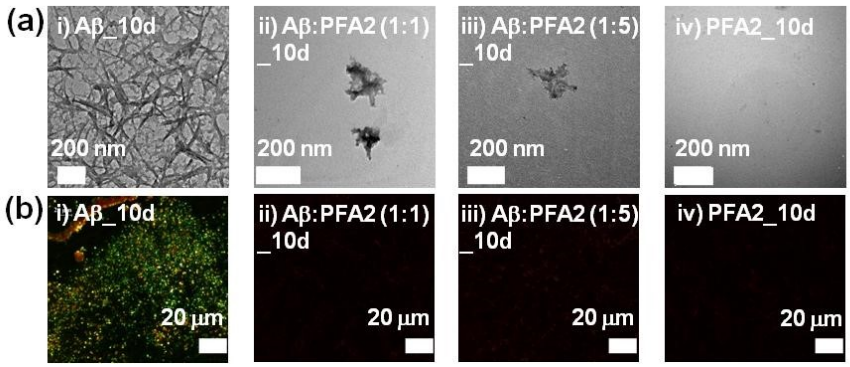

Figure S32. (a) TEM images, and (b) Congo red-stained birefringence images of $A\beta_{1-40}$ (i) in the absence, and presence of (ii) one-fold PFA2, (iii) five-fold PFA2, and (iv) PFA2 alone. Scale bars are indicated as 200 nm for TEM images, and 20 μm for birefringence images. All the peptide solutions were incubated in PBS pH 7.4 (50 mM) at 37 °C in parallel. All the images were captured after ten days of incubation.

Inhibition of amyloid accumulation of $A\beta_{1-40}$ by PFA3:

ThT fluorescence assay, CD experiments, and FTIR spectra of $A\beta_{1-40}$:

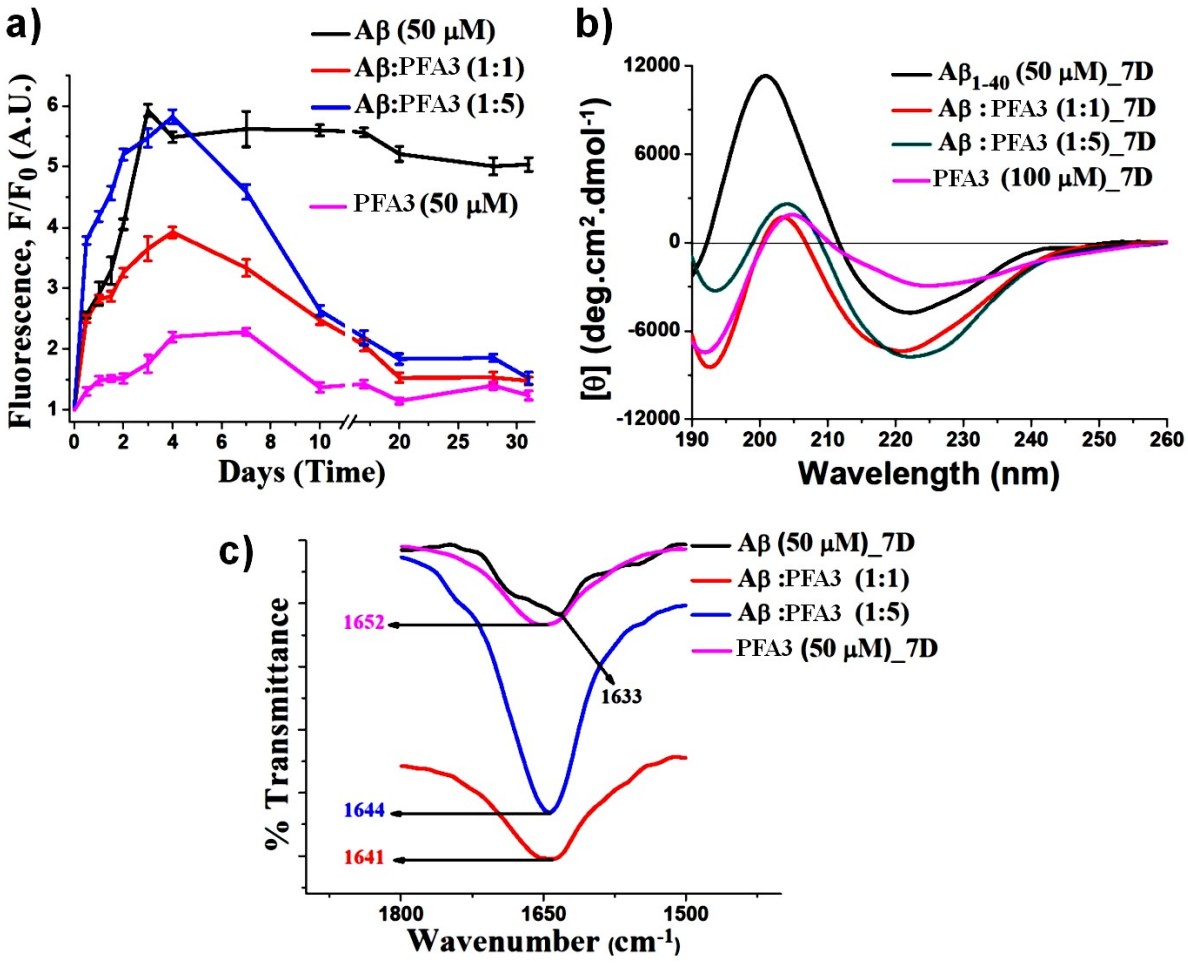

Figure S33. Normalized profiles of (a) dose-dependent ThT fluorescence assay. Spectra of $A\beta_{1-40}$ in the absence (black), presence of one-fold PFA3 (red), five-fold PFA3 (blue), and PFA3 alone (magenta). Error bars represent standard deviations of at least three independent measurements. (b) CD spectra of $A\beta_{1-40}$ in the absence and presence of PFA3 after seven days of incubation. Spectra of $A\beta_{1-40}$ in the absence (black), presence of one-fold PFA3 (red), five-fold PFA3 (dark cyan), and PFA3 alone (magenta). (c) FTIR spectra of $A\beta_{1-40}$ in the absence and presence of PFA1 after seven days of incubation. Spectra of $A\beta_{1-40}$ in the absence (black), presence of one-fold (red) PFA3, five-fold PFA3 (blue), and PFA3 alone (magenta). All the peptide solutions were incubated in PBS pH 7.4 (50 mM) at 37 °C.

TEM images, and Congo red-stained birefringence images of amyloid fibrils formed by $A\beta_{1-40}$:

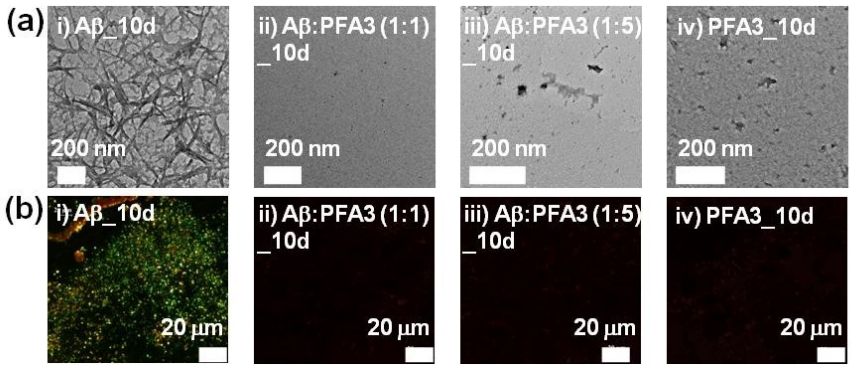

Figure S34. (a) TEM images, and (b) Congo red-stained birefringence images of $A\beta_{1-40}$ (i) in the absence, and presence of (ii) one-fold PFA3, (iii) five-fold PFA3, and (iv) PFA3 alone. Scale bars are indicated as 200 nm for TEM images, and 20 μm for birefringence images. All the peptide solutions were incubated in PBS pH 7.4 (50 mM) at 37 °C in parallel. All the images were captured after ten days of incubation.

Disruption of fibrillar amyloid of $A\beta_{1-40}$ by PFAs:

ThT fluorescence assay, FTIR spectra, TEM images, and Congo red-stained birefringence images of $A\beta_{1-40}$:

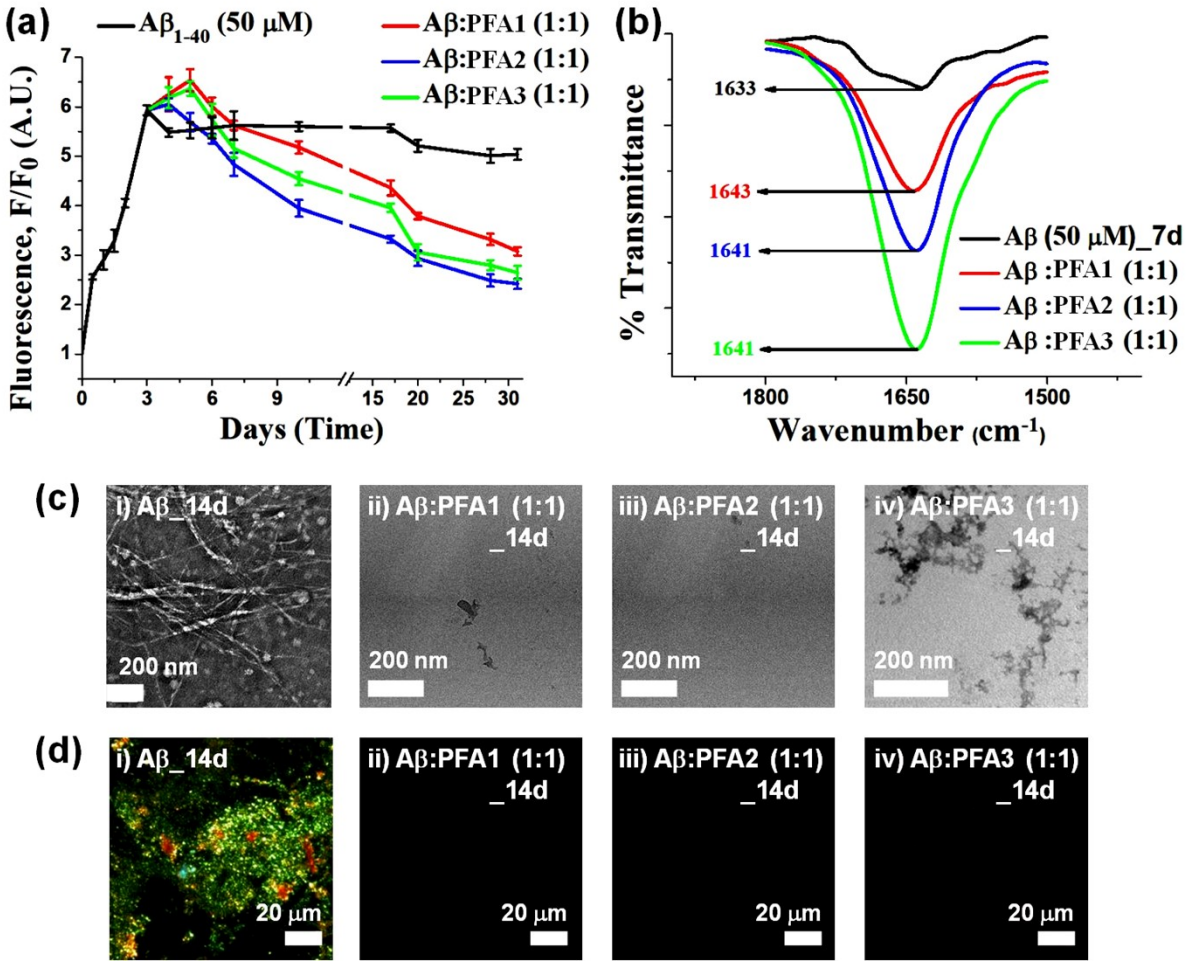

Figure S35. Normalized profiles of (a) time-dependent ThT fluorescence assay, and (b) FTIR spectra where PFAs were added after three days to the preformed fibril of $A\beta_{1-40}$. (a-b) Spectra of $A\beta_{1-40}$ in the absence (black), presence of one-fold PFA1 (red), one-fold PFA2 (blue), and one-fold PFA3 (light green). Error bars represent standard deviations of at least three independent measurements. (c) TEM images, and (d) Congo red-stained birefringence images of $A\beta_{1-40}$ (i) in the absence, and presence of (ii) one-fold PFA1, (iii) one-fold PFA2, and (iv) one-fold PFA3. Scale bars are indicated as 200 nm for TEM images, and 20 μm for birefringence images. All the images were captured after 14 days of incubation. All the peptide solutions were incubated in PBS pH 7.4 (50 mM) at 37 °C in parallel.

Characterization data:

Characterization details of mAβ and DTP28 were shown in the ESI (Fig. S87- S88, and Fig. S95- S96 respectively) of our published article (*ChemComm* **2020**, 56, 2348-2351).

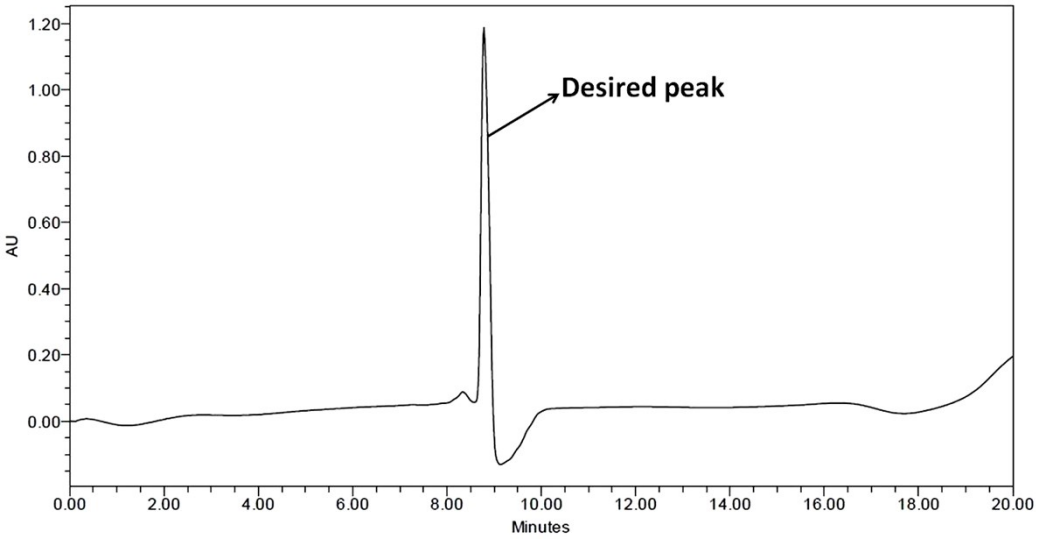

Figure S37. HPLC profile picture of the PFA1.

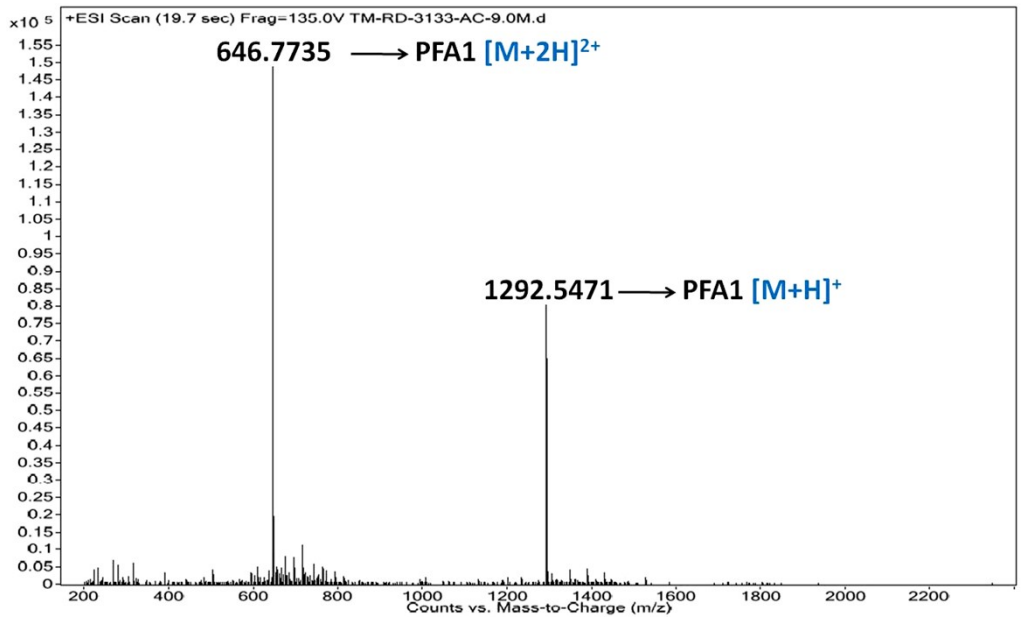

Figure S38. ESI-MS profile picture of purified PFA1. Calculated m/z for $C_{56}H_{77}N_{17}O_{17}S$ $[M+H]^+$ is 1292.5404, observed 1292.5471; Calculated m/z for $C_{56}H_{77}N_{17}O_{17}S$ $[M+2H]^{2+}$ is 646.7702, observed 646.7735.

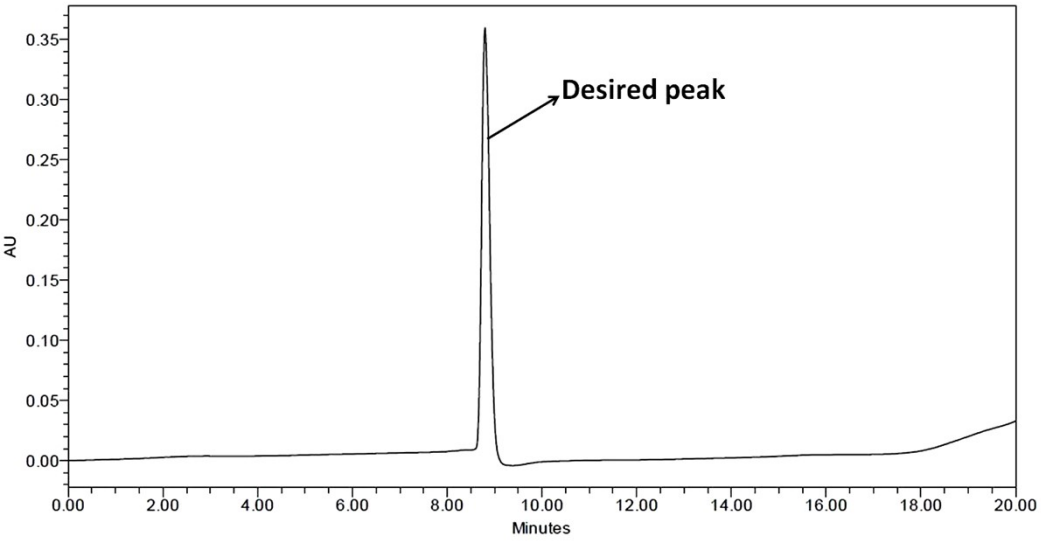

Figure S39. HPLC profile picture of the PFA2.

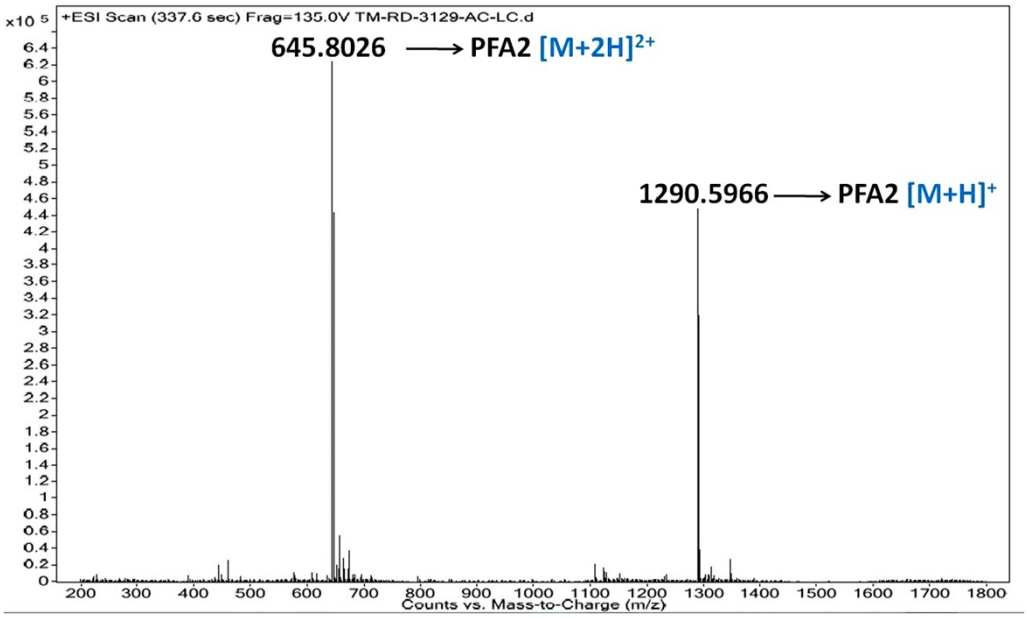

Figure S40. ESI-MS profile picture of purified PFA2. Calculated m/z for $C_{57}H_{79}N_{17}O_{18}$ $[M+H]^+$ is 1290.5789, observed 1290.5966; Calculated m/z for $C_{56}H_{77}N_{17}O_{17}S$ $[M+2H]^{2+}$ is 645.7894, observed 645.8026.

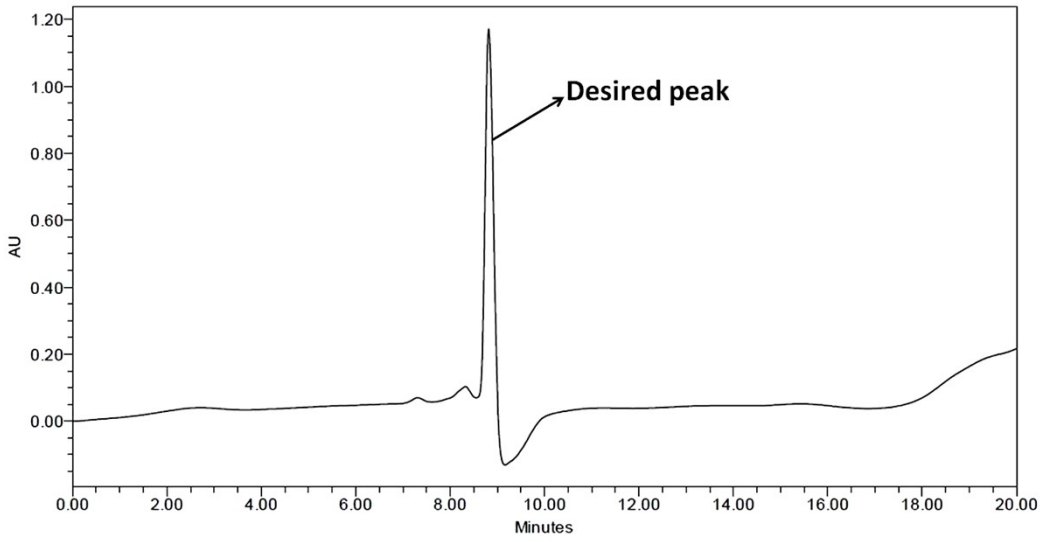

Figure S41. HPLC profile picture of the PFA3.

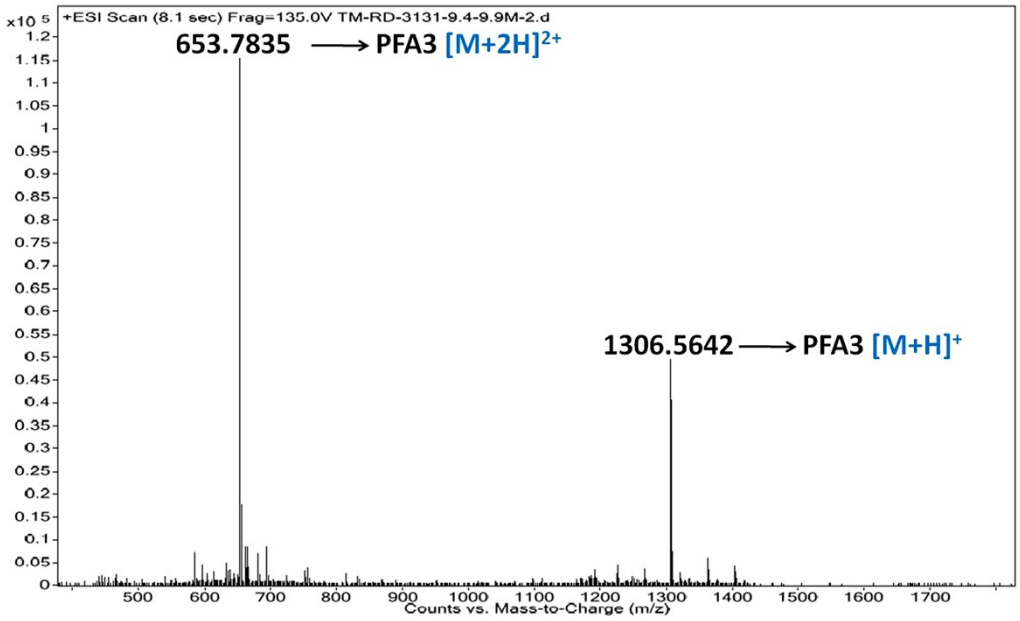

Figure S42. ESI-MS profile picture of purified PFA3. Calculated m/z for $C_{57}H_{79}N_{17}O_{17}S$ $[M+H]^+$ is 1306.5561, observed 1306.5642; Calculated m/z for $C_{56}H_{77}N_{17}O_{17}S$ $[M+2H]^{2+}$ is 653.7780, observed 653.7835.